ACS NANO

www.acsnano.org



REVIEW

# Functionalized Nanomaterials Capable of Crossing the Blood–Brain Barrier

Shuai Zha,[▽] Haitao Liu,[▽] Hengde Li, Haolan Li, Ka-Leung Wong,* and Angelo Homayoun All*

Cite This: *ACS Nano* 2024, 18, 1820–1845

Read Online

ACCESS | Metrics & More | Article Recommendations

**ABSTRACT:** The blood–brain barrier (BBB) is a specialized semipermeable structure that highly regulates exchanges between the central nervous system parenchyma and blood vessels. Thus, the BBB also prevents the passage of various forms of therapeutic agents, nanocarriers, and their cargos. Recently, many multidisciplinary studies focus on developing cargo-loaded nanoparticles (NPs) to overcome these challenges, which are emerging as safe and effective vehicles in neurotheranostics. In this Review, first we introduce the anatomical structure and physiological functions of the BBB. Second, we present the endogenous and exogenous transport mechanisms by which NPs cross the BBB. We report various forms of nanomaterials, carriers, and their cargos, with their detailed BBB uptake and permeability characteristics. Third, we describe the effect of regulating the size, shape, charge, and surface ligands of NPs that affect their BBB permeability, which can be exploited to enhance and promote neurotheranostics. We classify typical functionalized nanomaterials developed for BBB crossing. Fourth, we provide a comprehensive review of the recent progress in developing functional polymeric nanomaterials for applications in multimodal bioimaging, therapeutics, and drug delivery. Finally, we conclude by discussing existing challenges, directions, and future perspectives in employing functionalized nanomaterials for BBB crossing.

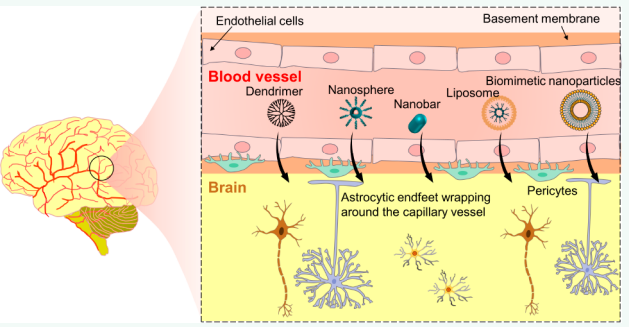


**KEYWORDS:** *functionalized nanomaterials, BBB crossing, receptor-mediated transcytosis, absorptive-mediated transcytosis, BBB receptor-mediated endocytosis, noninvasive BBB cargo delivery, central nervous system delivery, brain delivery, neurotheranostics*

## 1. INTRODUCTION

The interchange of biological materials that are indispensable for survival and function of neurons in the central nervous system (CNS) is well-controlled by the blood–brain barrier (BBB). The BBB is the largest interface for blood and brain exchanges. It establishes and maintains a very intricate equilibrium and homeostasis within the CNS parenchyma. Understandably, the structural integrity of the BBB is crucial for coherent function of the brain. Evidently, such superspecialized permeability constrains the therapeutic efficacy of many potential pharmacological agents that have been developed and could be used to treat neurological disorders as well. Recently, various methods of minimally invasive delivery have gained extensive attention and have become among the most prominent therapeutic strategies for CNS diseases. Nonetheless, any such strategy needs to overcome anatomical and physiological barriers in the CNS safely and effectively.[1]

The BBB is composed of endothelial cells, pericytes, astrocytes, and basement membrane, which form a highly selective semipermeable membrane. The main function of the BBB is to regulate the exchange of substances between the blood and the CNS based on brain physiological needs. Briefly, the BBB shields the CNS from toxins, pathogens, and foreign substances in the blood. It is also the gateway to supply the brain tissues with nutrients and expel unnecessary materials from the brain back into the bloodstream. The BBB establishes a very delicate ion homeostasis and adjusts the level of neurotransmitters, which guarantee impeccable function of the CNS.[2] Understandably, this peculiar superselective barrier also prevents blood circulating macromolecules such as recombinant proteins, antibodies, and nucleic acids,[3] as well as micromolecules, like trastuzumab,[4] doxorubicin,[5] or vincristine,[6] from entering into the brain parenchyma. However, development of nanotechnology has made significant break-

Received: October 30, 2023
Revised: December 20, 2023
Accepted: December 22, 2023
Published: January 9, 2024

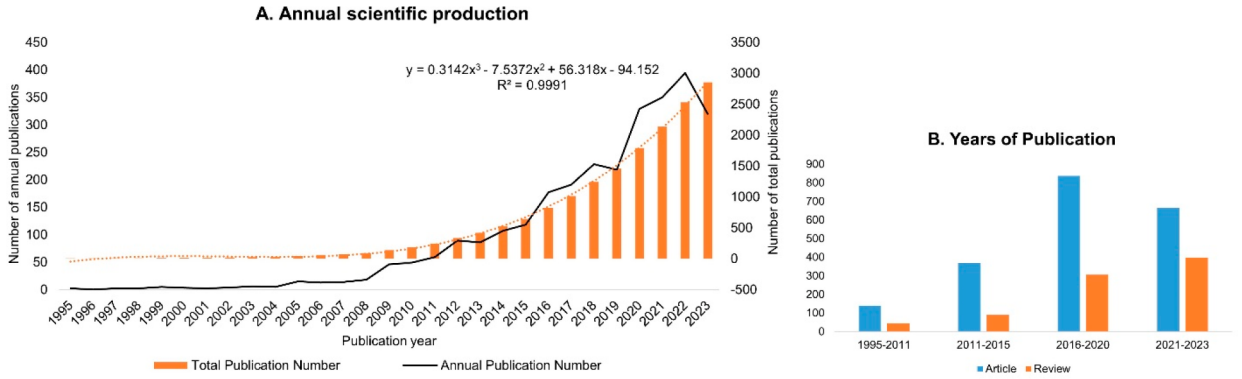


**Figure 1. Number of publications on nanoparticles crossing the BBB: Number of publications containing the terms ("nanoparticle*" OR "nanomaterial*" OR "nanocarrier*") AND ("BBB" OR "blood*brain*barrier") since 1995. (A) Annual number of articles, reviews, and proceedings was analyzed. The orange box plot represents total number of publications; the orange dashed line represents the trendline, and the black line represents the annual number of publications. (B) Number of published articles and reviews on functionalized nanoparticles crossing the BBB from 1995 to 2023. Blue bars represent published articles, and orange bars represent published reviews. Source: Web of Science, as assessed in October 2023. Note that papers in the categories "instruments instrumentation", "metallurgy metallurgical engineering", "robotics", "energy fuels", and "engineering mechanical" were excluded.**

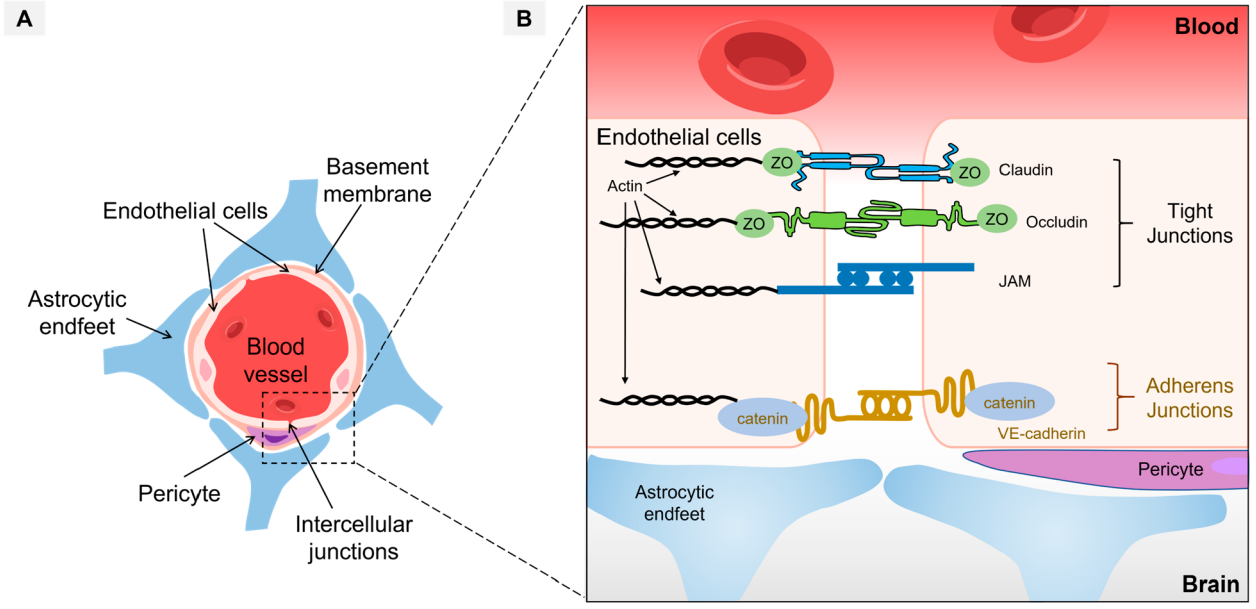


**Figure 2. Blood–brain barrier (BBB) and intercellular junctions between endothelial cells. (A) Structures of the BBB, which is composed of the endothelial cells, pericytes, basement membrane, and astrocytes; (B) Schematic of brain endothelial connections, including tight junctions, gap junctions, and adherens junctions. Reproduced with permission under a Creative Commons License from ref 21. Copyright 2021 the Authors, published by Springer Nature.**

throughs in creating reliable gates through the BBB.[7] Since, nanomaterials can also deliver loaded agents (drugs, genes, etc.), they have been exploited as multifunctional delivery systems to the CNS due to their innocuous ability to cross the BBB.[8]

Nanomaterials like inorganic nanoparticles, liposomes, dendrimers, and polymers have gained extensive attention in the field of drug and gene delivery, due to their incomparable advantages, such as higher drug loading capacity, lower dose and administration frequency, good biocompatibility (less side effects), high stability, enhanced bioavailability and biodegradability, targeted applications with less invasive theranostic techniques, decreased acquired drug resistance, negligible toxicity and immunogenicity, reduced off-target toxicity, feasibility for various routes of administration (intranasal, oral, and intravenous, and intramuscular injection), sustained and controlled drug release, unique properties (physical, electronic, chemical, and optical), and effective tracing of drug delivery.[3,9] These nanomaterials are being designed and developed as safe, effective, feasible, and practical tools for diagnosing and treating diseases of the CNS.[10] The current interest in functionalized NPs crossing the BBB is reflected in the number of publications per year, which showed a relatively stable growth trend between 1995 and 2023 in general (Figure 1A). Papers published in the last 3 years account for 37% of the total number. According to the quantitative analysis of the chart, a growth trend was revealed in the past few decades in global original research, from 140 articles between 1995 and 2011 to 837 articles from 2016 to 2020 and 666 articles in the past three years (2021–2023). In addition, the research results indicate that functionalized NPs crossing the BBB have attained increasing attention and discussion, from 46 reviews


https://doi.org/10.1021/acsnano.3c10674
ACS Nano 2024, 18, 1820–1845

during 1997−2011 to 306 reviews in 2016−2020 and 398 reviews in just 2021−2023 (Figure 1B). This rapid growth in published reviews highlights the emerging promise yet continued challenges of brain drug delivery using NPs. In this context, this review article first introduces the anatomical structure and physiological function of the BBB and then expounds on the challenges of BBB crossing, describing recent discoveries and innovative solutions. The mechanisms for BBB crossing of various nanomaterials and their cargos are also explained. Moreover, we highlight the advantages of implementing nanomaterials as carriers for drug delivery to the CNS via BBB crossing and the latest progress in these fields.

## 2. ANATOMICAL STRUCTURE OF INTACT BBB

The BBB is composed of microvascular endothelial cells, pericytes, and basement membrane from one side and long foot shaped extensions of astrocytes from the other side, forming an intimate association of end-feet protrusions of astrocytes that wrap around the endothelial cells of the capillary microvascular (Figure 2A).[11,12]

**2.1. Endothelial Cells.** Endothelial cells (ECs) are the basic building blocks of the BBB endothelium and are characterized by a flattened appearance in the inner layer.[13] They differ morphologically and metabolically from those in other mammalian capillary endothelia, containing a higher concentration of mitochondria and no fenestrations, forming a physically restrictive barrier by intercellular junctions.[14] The cerebral ECs have very few pinocytotic vesicles, yet they transport nutrients from the blood to the brain mainly via energy-dependent (produced by mitochondria) active transport. The BBB permeability can be altered or disrupted by mitochondria loss or any other dysfunction in the cerebral ECs.[15,16] In addition, the cerebral ECs offer an enzymatic barrier due to the presence of proteolytic enzymes including $\gamma$-glutamyl transpeptidase, alkaline phosphatase, and aromatic acid decarboxylase. This enzymatic barrier takes part in the assimilation of the neuroactive blood-borne solutes and drugs.[17]

**2.2. Pericytes and Vascular Basement Membrane.** Pericytes (PCs) and vascular basement membrane (BM) lie in the middle layer of the BBB. PCs are partly embedded within the BM and make peg-and-socket junctions with ECs through adhesion molecules.[18] These peg−socket junctions are formed where the BM is missing and act as anchors in which either pericytes or endothelial cell cytoplasmic projections (peg) lock into introversions (socket) of the other component.

**2.3. Astrocytes.** Astrocytes are the most abundant glial cells in the CNS. They are star-shaped and possess fine dendrite-like structures. At the end of these dendritic processes, there are small swellings called foot processes. There are two types of astrocytes: protoplasmic (located in the gray matter) and fibrous (located in the white matter). Astrocytes are the primary supporting cells of the nervous system, providing structural and metabolic support to the neurons, and have a vital role in tissue repair processes in the CNS. Interestingly, astrocytes also participate in the formation of tight junctions between cells lining the capillaries in the brain, resulting in the formation of the BBB membrane.[19] Clearly, any dysfunction or malfunction of astrocytes would lead to the obliteration of tight junction protein expression and leakage of substances.[20]

**2.4. Junctions at the Blood−Brain Barrier.** Brain ECs are closely connected by two distinct types of junctions: tight junctions and adherens junctions (Figure 2B).[21] Tight junctions consist of many different proteins in the cerebral microvasculature, including specific transmembrane and intracellular proteins. The transmembrane proteins comprise junction adhesion molecules (JAMs), claudins 1, 3, 5, and 12, and occludins, and the intracellular proteins include zonula occludens-1 (ZO-1). Adherens junctions are formed by cadherins (VE-cadherin or cadherin-5) and catenins, which are present at the basal side of EC−EC contacts. The primary mechanical role of catenins is to connect cadherins to actin filaments.[22] Furthermore, the endothelial Wnt/$\beta$-catenin pathway has been found to be one of the major molecular drivers of barriergenesis in the brain.[23,24] Hussain et al.[25] demonstrated the importance of $\beta$-catenin in maintaining BBB integrity using endothelial-specific $\beta$-catenin conditional knockout mice. These mice exhibited severe leakage of plasma proteins IgG and albumin into the cerebral cortex. This breakdown of the BBB was attributed to both paracellular and transcellular transport dysfunction. Mechanistically, the loss of $\beta$-catenin led to downregulation of TJ proteins, physical disruption of intercellular junctions, decreased expression of Mfsd2a (an inhibitor of transcytosis), and increased caveolin-1 (a protein associated with endocytosis).[25]

Owing to their components and biological functions, tight junctions and adherens junctions together maintain microvascular integrity and control the transport of molecules.[26] However, the restrictive properties of the BBB prevent most therapeutic agents from entering the brain parenchyma from the blood capillary vasculature. Approximately 98% of small molecules and nearly all large pharmacological and other molecules, such as polypeptides, antibodies, or oligonucleotides, cannot cross the BBB.[27] The protective function of the BBB is also one of the major limitations in drug delivery into the CNS and treatment.

## 3. ABNORMAL BBB STRUCTURE IN CNS DISEASES

BBB disruption typically involves degradation or shrinkage of ECs and altered paracellular transport pathways through reduced expression of TJ proteins and/or TJ translocations.[28] In addition, the expression or function of BBB-associated receptors and transport machinery may be affected, resulting in dysregulated molecular transport.[29] Importantly, disruption of the BBB may also involve different cellular components beyond the brain endothelium. These include pericyte degeneration or decreased pericyte coverage, basement membrane alterations,[30] and detachment of astrocyte terminal feet from the vascular basement membrane.[31] These astrocyte terminal podia may also exhibit a swollen phenotype under certain pathological conditions.[32] Besides, ECs can increase the expression of leukocyte adhesion molecules, leading to increased leukocyte extravasation into the brain parenchyma under pathological conditions.[33] These leukocyte−EC interactions can also directly contribute to the increased BBB permeability through the release of reactive oxygen species, cytokines, and other barrier-damaging mediators.[21] Understanding BBB dysfunction in CNS diseases may reveal opportunities for improvement in diagnosis, monitoring, and disease-modifying interventions.

**3.1. BBB in Stroke.** Stroke is a cerebrovascular disease that seriously threatens human health. There are two types of strokes: ischemic and hemorrhagic. Ischemic stroke accounts


https://doi.org/10.1021/acsnano.3c10674
ACS Nano 2024, 18, 1820−1845

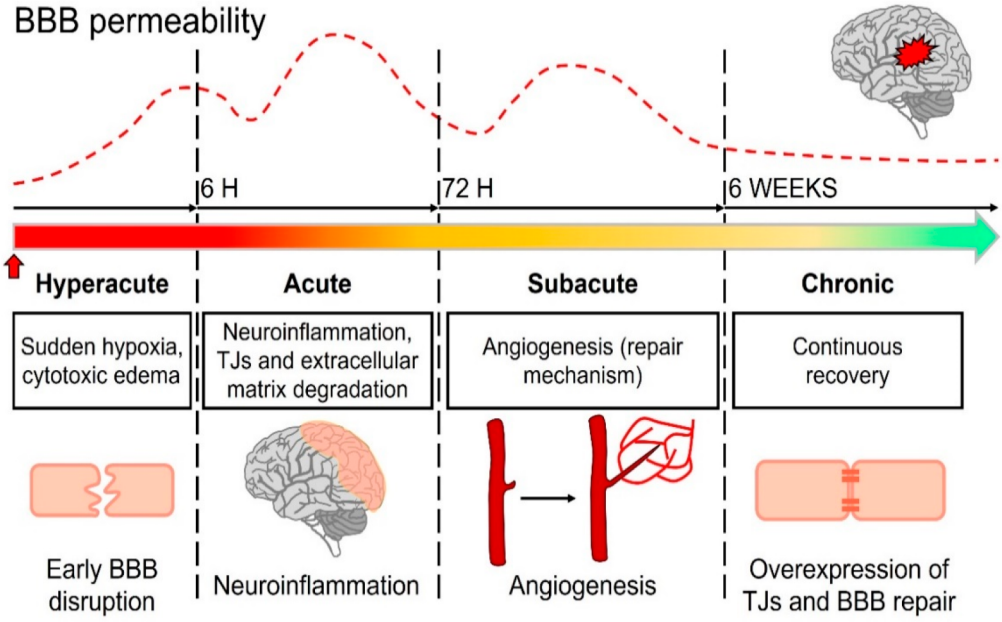


**Figure 3. Evolution of blood−brain barrier permeability in four phases of stroke and major pathophysiological processes in each phase. Early BBB disruption occurs in the hyperacute phase. The acute phase occurs thereafter, and neuroinflammation is a major factor in the development of injury. The subacute and chronic phases are characterized by repair processes, mainly angiogenesis and restoration of BBB. Reproduced with permission under a Creative Commons License from refs 37 and 39. Copyright 2020 and 2021 the Authors, published by Frontiers Media SA and Multidisciplinary Digital Publishing Institute.**

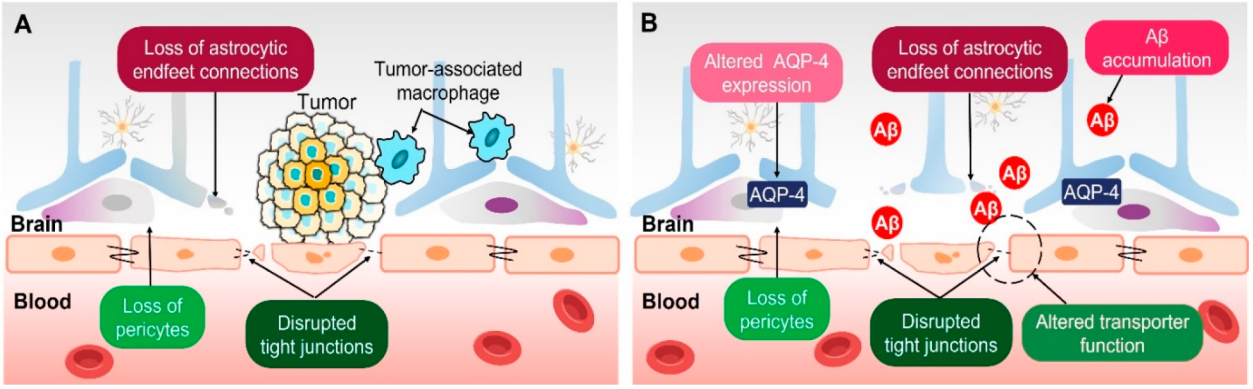


**Figure 4. Changes of blood−brain barrier in brain tumors and Alzheimer's disease. (A) Blood−brain tumor barrier (BBTB) characterized by abnormal and leaky blood vessels. Loss of tight junction proteins and astrocytic endfeet connections disrupts the integrity of the blood−brain barrier (BBB) and increases permeability. Reproduced with permission from ref 42. Copyright 2022 Wiley-Blackwell Publishing. (B) Changes in the blood−brain barrier (BBB) associated with Alzheimer's disease (AD). AD-specific changes in the BBB involve disruption of tight junctions and changes in transporters in brain ECs, degradation of pericytes, and altered expression of aquaporin-4 (AQP4) in astrocytes, thereby resulting in enhanced permeability. Consequently, these alterations are closely related to the accumulation of amyloid-$\beta$ (A$\beta$).**

for the majority of cases (80−87%).[34] BBB permeability appears to follow multiphasic patterns at different stroke stages that are associated with different biological substrates (Figure 3). In the hyperacute phase (first 6 h), sudden hypoxia disrupts the BBB, leading to cytotoxic edema, reactive oxygen species (ROS) generation, TJ and extracellular matrix degradation, and increased permeability; in the acute phase (6−72 h), the neuroinflammatory response exacerbates the BBB injury through the downregulation and degradation of TJs and extracellular matrix, gliosis, and EC activation, thereby causing increased permeability and subsequent hemorrhagic transformation risk by reperfusion therapy; in the subacute phase (72 h to 6 weeks), major repair mechanisms, such as angiogenesis, occur. Brain recovery and BBB permeability are closely associated with lesion volumes and stroke severity,[35] as well as neuroinflammation involving activated microglia and inflammatory cytokines. Bernardo-Castro et al.[36] (2023) found that BBB permeability was highest at 3−10 days poststroke possibly due to regenerative mechanisms, such as vascular remodeling, and this time window of increased permeability correlated with better clinical recovery.[35,36] During the chronic phase (>6 weeks), an increase in BBB restoration factors restores the barrier permeability through the overexpression of TJ proteins, reorganization of junction proteins, and secretion of neurotrophic factors.[37]

In short, BBB disruption, one of the major pathophysiological features of stroke, is closely associated with TJ dysfunction, endothelial injury, retraction of astrocytic endfeet,


https://doi.org/10.1021/acsnano.3c10674
ACS Nano 2024, 18, 1820−1845

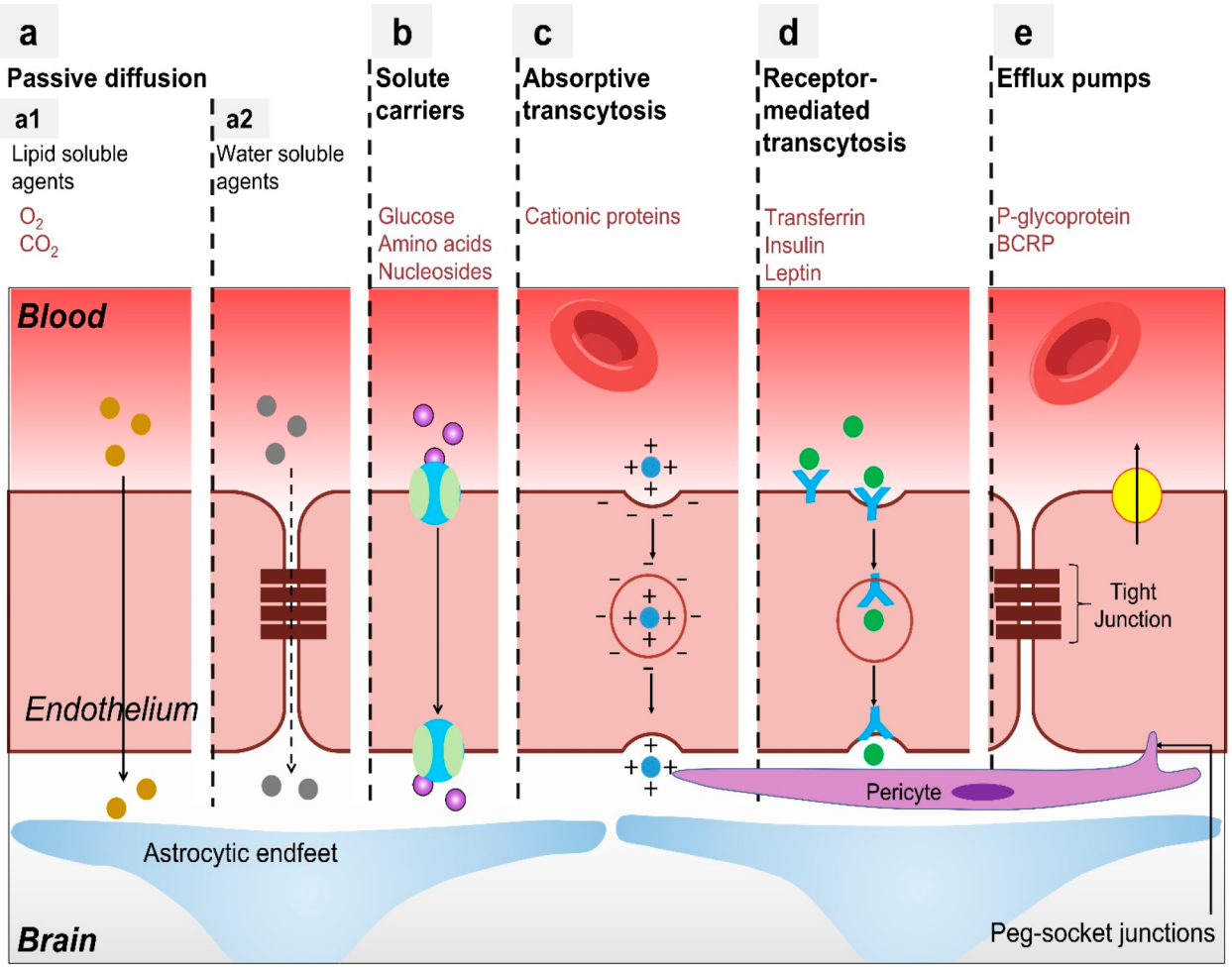


**Figure 5. Physiological transport mechanisms crossing the BBB. Different transport pathways are presented, including (A) passive diffusion, driven by a concentration gradient, mainly involving (A1) transcellular pathways and (A2) paracellular pathways, (B) solute carrier, as occurs for glucose, amino acids, and nucleosides, (C) absorptive-mediated transcytosis for transport of cationic proteins in a nonspecific manner, (D) receptor-mediated transcytosis for the transport of transferrin, insulin, and leptin, and (E) efflux pumps (in the case of P-glycoprotein and BCRP). Reproduced with permission from ref 71. Copyright 2014 Walter De Gruyter.**

and disruption of cell−cell interaction.[38] In the early phases of stroke, NPs can easily penetrate the brain due to the high permeability of the injured BBB. In the chronic phase, vasculogenesis usually occurs along with partial restoration of BBB integrity, therefore impairing NP transport through leaky vessels.[39]

**3.2. BBB in Brain Tumors.** The blood−brain tumor barrier (BBTB) undergoes distinct structural and functional changes compared to the intact BBB in healthy brain tissue (Figure 4A).[40] In glioblastoma (GBM), disruption of the BBB primarily occurs in the core of the tumor, where microvascular proliferation leads to newly formed leaky blood vessels. In contrast, the BBB tends to remain relatively intact in the peripheral zones surrounding the brain tumor.[41] As the primary tumors proliferate, the neovascularization and intratumor blood vessels will deteriorate, causing damage to the BBB, whose structure and function become very different from those of the healthy BBB; this is called the BBTB. As a consequence, microvessels of the brain tumors are classified into continuous and nonfenestrated capillaries, continuous and fenestrated capillaries, and discontinuous (with or without fenestrations) capillaries based on their morphology. However, while often they are described as "leakier" than the BBB,[42] some studies find the BBTB capable of expressing active efflux transporters and maintaining barrier integrity.[43] Therefore, the leaky BBTB is highly heterogeneous with wide variability in permeation[44−46] and abnormal tumor angiogenesis. This typically leads to a highly disorganized vasculature characterized by increased fenestrations and wider intercellular gaps that enhance paracellular transport. Tight junction proteins like claudin-3[47] and occludin[48] are frequently downregulated, further disrupting the barrier. Additionally, loss of pericytes, astrocyte endfeet connections,[49] and neuronal connections[50] could alter the BBTB microenvironment. BBTB permeability is also impacted by invading glioma cells that can physically displace astrocytic endfeet. Molecular transport changes are common, with upregulation of efflux pumps in the BBTB[51] but also increases in endothelial pinocytic transport vesicles that facilitate transcellular drug uptake.[51] Although the barrier still substantially limits delivery in many cases, these BBTB alterations result in enhanced penetration of chemotherapeutics, compared to that in the intact BBB. Increased immune cell infiltration is another characteristic of the BBTB change.[52] The disorganized and heterogeneous BBTB structure promotes leakage of blood products, a phenomenon known as the enhanced permeability and retention (EPR) effect, which is


https://doi.org/10.1021/acsnano.3c10674
ACS Nano 2024, 18, 1820−1845

typical in many cancerous tissues.[53] Overall, understanding the distinct properties of BBTB presents opportunities to develop strategies to safely and effectively overcome this barrier and improve drug delivery to brain tumors.

**3.3. BBB in Neurodegenerative Diseases.** *3.3.1. BBB in Alzheimer's Disease.* AD is a prevalent neurological disorder, recognized as the primary cause of dementia.[54] The initial occurrence associated with AD is the accumulation of A$\beta$, which can lead to cerebral amyloid angiopathy.[55] The buildup of A$\beta$ surrounding blood vessels has the potential to cause pericyte death[56] and altered astrocyte morphology,[57] consequently compromising BBB integrity (Figure 4B).[58] Another major pathology hallmark in AD is the presence of tau deposits.[57] Tau protein deposition also damages the vasculature, resulting in atrophic string capillaries and capillary surface irregularities.[59,60] Additional BBB alterations in AD include endothelial abnormalities like mitochondrial damage, disrupted tight junctions, extracellular matrix alteration,[30] reactive gliosis (early event in AD), molecular and functional changes in astrocytes, such as dysregulated potassium/calcium homeostasis and inflammation, reduced astrocyte metabolism (glycolysis and oxidative phosphorylation), astrocyte degeneration, increased aquaporin-4 expression in astrocytes,[61] pericyte loss and reduced coverage on ECs, and peripheral immune cell infiltration.[62] These widespread structural and functional changes to the neurovascular unit likely contribute to AD progression and cognitive decline.

*3.3.2. BBB in Parkinson's Disease.* Parkinson's disease (PD) is characterized by the loss of dopaminergic neurons in the substantia nigra pars compacta and the presence of Lewy bodies, which are intracellular inclusions mainly formed by insoluble $\alpha$-synuclein.[63] The aging brain undergoes decreased capillary density, decreased blood flow, and impaired barrier integrity.[64] In moderate-stage PD, an increase in vessel density indicates angiogenesis, while in late-stage disease, vessel density is significantly reduced, suggesting dynamic disease-stage-dependent vascular changes. Histological analyses have revealed capillary leakage, extravasated erythrocytes, perivascular hemosiderin deposits, and accumulation of serum proteins in PD patients.[65] Activated microglia are mostly localized around blood vessels. PD-associated astrocytes are pro-inflammatory and fail to support capillary formation *in vitro*.[66] Increased cerebrospinal fluid/serum ratios of albumin and IgG have also been reported in PD patients, indicating compromised BBB integrity.[67,68] Several studies have demonstrated BBB disruption in PD using imaging approaches. For example, Bartels et al. found increased brain uptake of [$^{11}$C]verapamil in PD patients, suggesting decreased P-glycoprotein efflux activity.[69] Furthermore, Al-Bachari et al. showed greater contrast agent transfer across the BBB in PD patients compared to healthy controls, reflecting increased BBB permeability.[70] Overall, substantial evidence points to BBB impairment as a critical pathophysiological component of PD.

## 4. BBB TRANSPORT MECHANISMS

The physiological functions of the BBB involve the maintenance of ionic homeostasis and brain nutrition, regulation of neurotransmitter levels, and protection of the brain from exogenous neurotoxins and plasma macromolecules. We describe the transport mechanisms of the BBB under physiological conditions, and the endogenous and exogenous permeation mechanisms yielding NP crossing of the BBB.

Despite the highly restrictive transport of substances across the BBB, the brain has substantial demands for nutrients and energy. Therefore, multiple mechanisms mediate brain uptake of specific endogenous substances through passive or active transport routes. Generally, substances may cross the BBB under physiological conditions by (i) passive diffusion, (ii) carrier-mediated transport, (iii) adsorptive-mediated transcytosis, (iv) receptor-mediated transport, and (v) efflux pumps (Figure 5).[71]

**4.1. Transport via Simple Diffusion.** Passive transport is a nonspecific, energy-independent, concentration-dependent transport process that is limited to small molecules. In general, it can be categorized into paracellular and transcellular diffusion patterns. The presence of tight junctions (TJs) renders the intercellular space extremely narrow, thus physically hindering paracellular transport across the BBB. However, small lipophilic molecules, with a molecular weight <400−500 Da and a number of hydrogen bonds <8−10, may enter the brain through lipid-mediated free diffusion.[11] In addition, small gaseous molecules such as $O_2$ and $CO_2$ rapidly and freely diffuse between the blood and the brain parenchyma.[21]

**4.2. Carrier-Mediated Transport.** Carrier-mediated transport is one of the most prevalent transport mechanisms across BBB, where nutrients, such as glucose, amino acids, and nucleosides, are transported.[72] It can be classified as facilitated transportation or secondary active transport. The facilitated transportation does not require energy since it is driven by electrochemical or concentration gradients. However, secondary active transport means the transport of a solute in the direction of its increasing electrochemical potential coupled with facilitated diffusion. These solute carriers may be specific to one molecule or to several molecules. By this path, the nutrient molecule first binds to the specific transporter at the luminal side. Then the transporter changes its conformation to transfer it into the brain parenchyma.

**4.3. Adsorptive-Mediated Transcytosis.** Adsorptive-mediated transcytosis (AMT) is induced by electrostatic interactions between positively charged cationic molecules and negatively charged membrane surface domains,[73] causing cell membrane invagination and vesicle formation primarily through negatively charged clathrin-coated pits and through caveolae.[74] The EC membrane is covered by a glycocalyx, composed of heparan sulfate proteoglycans (HSPGs). HSPGs contain one or more covalently attached highly negatively charged heparan sulfate chains. Additionally, the sialoglycoproteins and sialoglycolipids contribute to a negative surface charge on the BBB. These factors work together to make the BBB luminal side highly negatively charged.[75] Therefore, cationic molecules can be transferred into the brain parenchyma through interaction with the negatively charged surface of the cell membrane, such as cationic proteins.

**4.4. Receptor-Mediated Transcytosis.** Receptor-mediated transcytosis (RMT) is the main pathway to transport large molecules across the BBB. It is used to transport components like iron, insulin, and leptin in a homeostatic manner,[76] as their receptors are highly expressed on the luminal surface of the BBB. It usually initiates with the binding of ligands with specific receptors on the luminal surface of the ECs, subsequently triggering membrane invagination and endocytosis. Intracellular transport vesicles involve either clathrin- or caveolae-mediated mechanisms.[77] Clathrin-mediated endocytosis is characterized by the formation of "clathrin coat", a polyhedral structure (clathrin triskelion). The adaptor protein


https://doi.org/10.1021/acsnano.3c10674
ACS Nano 2024, 18, 1820−1845

**Table 1. Nanoparticle System-Based Drug Delivery through Endogenous Transport Mechanisms**

| transport mechanism | uptake mechanism | size (nm) | zeta potential (mV) | target model of the BBB | ref |
|---|---|---|---|---|---|
| simple diffusion | diffusion | 2.28 ± 0.32 | [a] | spheroids | 85 |
| | direct passage by ion channels | 2.5 | [a] | rats | 86 |
| carrier mediated transcytosis | glucose transporter (GLUT) | 118 | [a] | APP/PS1 mice | 103 |
| | | 178.5 ± 2.3 | 15.5 ± 1.3 | bEnd.l/3 cells and mice | 104 |
| | | 172.0 ± 3.7 | 13.5 ± 0.7 | | |
| | large neutral amino-acid transporter 1 (LAT-1) | 89.6 ± 4.1 | −34.6 ± 1.0 | hCMEC/D3 cells and primary rat brain ECs | 105 |
| | | 385 ± 21 | 0.554 ± 0.110 | rats | 106 |
| absorptive mediated transcytosis | electrostatic interaction | 156 ± 10.85 | 22 ± 2.1 | bEnd.3 cells | 107 |
| | | 82.1 ± 9.3 | 20.3 ± 3.7 | hCMEC/D3 cells | 108 |
| | | 261 ± 8 | 45 ± 1 | hCMEC/D3 cells | 109 |
| receptor mediated transcytosis | transferrin receptor (TfR) | 6.612 ± 0.8893 (radius) | [a] | bEnd.3 cells, hCMEC/D3 cells, and glioma-bearing mice | 110 |
| | lactoferrin receptor (LfR) | [a] | [a] | human HBEC-5i cells | 111 |
| | | [a] | [a] | | |
| | low-density lipoprotein (LDL) receptor family | [a] | 19 | mouse brain ECs and APP/PS1 AD mice | 112 |
| | | 57.7−107.7 | −3.6 (fresh) | bEnd.3 cells, mice and brain metastasis-bearing mice | 113 |
| | high-density lipoprotein receptor (HDLR) | [a] | [a] | HBMECs | 114 |
| | $\alpha_v\beta_3$ integrin | 192 ± 7 | [a] | hCMEC/D3 cells, bEnd.3 cells, and glioma-bearing mice | 115 |
| efflux pump | P-gp | 482.4 ± 33.0 | −41.2 ± 2.7 | hCMEC/D3 cells | 116 |
| | P-gp | ∼105 | −10.1 | hCMEC/D3 cells | 117 |

[a]Not applicable.

**Table 2. Nanoparticle System-Based Drug Delivery through Exogenous Transport Mechanisms**

| interference agents | penetration mechanism | targeted disease | target model of BBB | ref |
|---|---|---|---|---|
| osmotic agents | osmotic opening | [a] | mice | 119 |
| focused ultrasound (FUS) | interaction of FUS with injected microbubbles | Alzheimer's disease | APP/PS1 mice, BALB/c mice | 144 |
| laser | tight junctions (TJs) | [a] | mice | 130 |
| magnetic field force | influence of the magnetic field | [a] | HBMECs | 133 |
| | influence of the hyperpermeability of the tumor vasculature and magnetic field | glioma | glioma-bearing rats | 134 |
| cell-mediated transcytosis | response to brain inflammation | glioblastoma (GBM) | bEnd.3 cells and GBM bearing mice | 143 |

[a]Not applicable.

AP2 initiates the clathrin assembly and the recruitment of other accessory proteins. Once completed, dynamin and other adaptor proteins separate clathrin-coated vesicles from the cell membrane through scission. Then, the clathrin coat will be rapidly removed and the internalized vesicle is free and primed to be trafficked and fused with an early endosome.[78] This is the main transport mechanism of numerous endogenous substances, such as transferrin (Tf). Caveolae-mediated endocytosis and trafficking are also involved in the transport of lipids and fatty acids in ECs, by forming a small flask-shaped depression of plasma membrane, composed of phospholipids, sphingolipids, and cholesterol[79] in the following steps: (1) budding and detachment from the cell membrane, (2a) fusion with endosomes followed by accumulation into lysosomes (classic), (2b) non-endosomal trafficking to intracellular organelles, or (2c) transporting substances from the bloodstream to tissues as a transcellular carrier (in endothelia), and (3) recycling of caveolae.[80]

**4.5. Transport via Efflux Pumps.** Efflux pumps are proteins localized on the endothelial membrane and use ATP hydrolysis to translocate solutes across the cellular membrane. Therefore, they can force the efflux of solutes against a concentration gradient. They are important machinery for expelling unwanted solutes into the capillary lumen. The principal efflux pumps in the BBB include P-glycoprotein (P-gp), breast cancer resistance protein (BCRP), and multidrug resistance-associated proteins.[81] The inhibition of efflux pumps is another potential strategy for cargo delivery through the BBB and into the CNS parenchyma.

## 5. PERMEATION MECHANISMS OF NANOPARTICLES CAPABLE OF CROSSING THE BBB

NPs have been widely developed to deliver therapeutic agents through the BBB via endogenous or exogenous transport mechanisms. NPs can be functionalized to hijack the transport mechanism of endogenous substances (glucose and transferrin, Table 1) or cross through temporary BBB disruption exploiting exogenous effects (mannitol or focused ultrasound, Table 2).

**5.1. Endogenous Transport Mechanisms of Nanoparticles Capable of Crossing the BBB.** *5.1.1. Passive Diffusion.* The TJs between ECs have a gap of 4−6 nm,[82] which allows the particles smaller than 4 nm to cross the BBB through passive diffusion. First, small NPs like gold nanoparticles (AuNPs)[83] and carbon dots (CDs) or lipid-based


https://doi.org/10.1021/acsnano.3c10674
ACS Nano 2024, 18, 1820−1845

formulations may freely cross the BBB via passive diffusion. AuNPs are clustered particles with sizes ranging from 1 to 100 nm consisting of a gold core and a surface coating.[84] When dispersed in a fluid, usually water, they are known as colloidal gold. Their small size allows them to cross biological barriers, e.g., the BBB. Sokolova et al.[85] observed that the concentration of ∼2 nm core diameter AuNPs increased over time inside the spheroid (an *in vitro* BBB model) conceivably by the passive diffusion mechanism. Spheroids have been developed as *in vitro* BBB models, demonstrating typical restrictive permeability and comprising various brain cells including astrocytes, neurons, microglia, oligodendrocytes, pericytes, and a surface layer of endothelial cells. Using these spheroid models, time-dependent accumulation of AuNPs in the spheroid core was observed after 30 min, 6 h, and 24 h of incubation.[85] Sela et al.[86] synthesized 1.3 ± 0.3 nm AuNPs and found apparent accumulation in the frontal cortex, hippocampus, and hypothalamus of rats 6−16 h after intra-abdominal injection (200 μL, 105 mg/L). However, it was also noticed that AuNP crossing from capillaries into the brain parenchyma may be mediated by ion channels. $Ca^{2+}$, $Na^{+}$, and $K^{+}$ channel blockers halved the concentration of AuNPs crossing the BBB compared to the corresponding value found in the control rats. This was explained by two possible mechanisms: (1) the blockers reduce the direct passage of AuNPs through the ion channels, where the diameters of $Ca^{2+}$, $Na^{+}$, and $K^{+}$ are in the range of 0.9−1.5 nm, comparable to the size of the AuNPs, or (2) the blockers affect the ionic balance and lead to a reduction in BBB permeability through the TJs, therefore reducing the AuNP transfer.[86]

CDs are carbon-based core−shell NPs with low toxicity due to their lack of metals. They can penetrate the BBB by passive diffusion due to their small particle sizes (1−10 nm), low surface charge, and amphiphilicity.[87,88] Zhou et al. found that CDs could cross the BBB due to their unique properties, including small size (3.4 ± 1.0 nm), low zeta potential (−15.3 mV), and amphiphilicity. CDs accumulated in the brains of zebrafish after 12 h of soaking, likely due to amphiphilicity.[89] Carbon nitride dots under 2 nm also crossed the BBB through passive diffusion, as seen by their appearance in the central canal of zebrafish spinal cord 10 min after intravascular injection.[88] Deng et al. showed that ∼2 nm amphiphilic CDs could cross the BBB with 10−20% efficiency *in vitro*. Furthermore, guanidine groups were introduced to CDs to interact with anionic TJs via cationic charge.[90] Overall, these studies demonstrate that CDs are a promising NP platform for enhanced BBB permeation through passive diffusion. In addition, lipid-based carriers, such as solid lipid nanoparticles (SLNs) and nanostructured lipid carriers (NLCs), can penetrate across the BBB and be translocated in the brain through passive diffusion due to the lipid nature of the BBB[91,92] and the nanometric size (40−200 nm).[93] They are promising lipid-based formulations to treat CNS diseases. SLNs are prepared using solid lipids, such as mono-, di-, and triglycerides, fatty acids, waxes, and steroids. Adding various physiologically compatible emulsifiers, i.e., phospholipids, poloxamers, and polysorbates, also stabilizes NP formulations. Similarly, NLCs are modified SLNs in which the lipid phase consists of liquid lipids (oils) and solids at room temperature.[94] The small size and lipid nature of SLNs and NLCs facilitate crossing the BBB, especially in the leaky tumor vasculature.[95,96] Regarding drug delivery to the CNS, both SLNs and NLCs have been confirmed to improve the treatment of several neurological diseases, such as Parkinson's disease,[97] Alzheimer's disease,[98] migraine, epilepsy, and brain cancer.[92] Many studies demonstrated the superiority of NLCs and SLNs over other nanoparticles (e.g., PLGA NPs[99]) to promote targeted delivery of drugs to the brain due to their lipid properties.[100−102]

*5.1.2. Carrier-Mediated Transport.* The most explored carriers on ECs that are targeted for transporting NPs across the BBB are glucose transporters (GLUTs) and the L-type amino acid transporter (LAT). Zhou et al. reported that galactose-conjugated NPs can be delivered into APP/PS1 transgenic AD mice through the interaction with GLUT1 on ECs.[103] Arora et al. found that dual modification with mannose (through GLUT1) and penetrating peptides in the liposomes can promote selectivity and enhance prospective delivery to the brain.[104] Besides, LAT-1 is utilized as the target carrier for L-DOPA or L-valine conjugated NPs and enhances their entrance into the brain.[105,106]

*5.1.3. Adsorptive-Mediated Transcytosis.* NPs could be functionalized with cationic components to enhance electrostatic interaction with the anionic surface of endothelial cells in order to facilitate their adsorptive-mediated transcytosis. Muniswamy et al. discovered that "dendrimer-cationized-albumin" encrusted NPs presented superior permeation transport across monolayer mouse brain endothelial bEnd.3 cells.[107] Likewise, drug-loaded cationic liposomes (CLPs) could cross the immortalized human brain microvascular endothelial (hCMEC/D3) monolayer cells (*in vitro* BBB model).[108] Chitosan-coated human serum albumin NPs can also interact with negatively charged cell membranes, subsequently crossing into hCMEC/D3 cells, accompanied by reversible and transient tight junction opening between the cells.[109] Positively charged NPs offer superior efficacy of drugs in the CNS models while significantly improving BBB permeation. Hence, they could be ideal candidates for cargo delivery to the brain.

*5.1.4. Receptor-Mediated Transcytosis.* Typically, for receptor-mediated transcytosis, NPs are conjugated with specific ligands. Fan et al. showed that H-ferritin (HFn) is an ideal ligand for conjugated-NPs to cross the intact BBB.[110] Similarly, lactoferrin,[111] angiopoietin-2,[112,113] apolipoprotein A1,[114] and cRGD[115] were also conjugated with NPs to facilitate their penetration into the brain parenchyma. Ligand-modified NPs show excellent BBB crossing ability through the interaction with receptors expressed on healthy brain ECs. Interestingly, some ligand-modified NPs also show dual targeting abilities (BBB traversing and targeting the brain lesion) because the ligands on the NP surface can also bind to receptors expressed on abnormal brain cells. Therefore, these NPs may possess great potential to serve as an approach to BBB crossing as well as CNS selective treatments.

*5.1.5. Efflux Pump Inhibitors.* The most explored efflux pump present on cerebral ECs is P-gp. Specific P-gp inhibitors have been used as a strategy for reducing the efflux of NPs and enhancing their entry into the brain. For instance, Gomes et al. revealed that reducing P-gp expression by siRNA NPs could enhance P-gp substrate permeability via modulating drug efflux at the BBB.[116] Similarly, PEGylated PLGA NPs were applied to transport coumarin C75 for the treatment of PD, most probably via the inhibition of the P-gp efflux pump in hCMEC/D3 cells.[117] The BBB-targeted NP induced P-gp down-regulation and consequently increased P-gp substrate


https://doi.org/10.1021/acsnano.3c10674
ACS Nano 2024, 18, 1820−1845

permeability across brain membranes would allow for successful influx of drugs across the BBB.

In conclusion, passive diffusion can only be employed in some ultrasmall NPs, usually with a size of less than 4 nm. Their surface might also be modified to enhance the BBB crossing through specific modification methods, e.g., positive charge, ligands, or antibodies.[82] Other passive and active mechanisms could also be responsible for the active transportation of molecules. Indeed, some of these mechanisms are exploited for the delivery of NP-conjugated drug(s) into the brain through the "Trojan horse" strategy. Their conjugation with targeting moieties can directly target brain endothelium and facilitate the internalization of cargos via endocytosis or transcytosis. Among these, (i) carrier-mediated transporters, (ii) adsorptive-mediated endocytosis, (iii) receptor-mediated endocytosis, and (iv) active efflux transporters are the most explored models for NP delivery in treating brain diseases.

**5.2. Exogenous Transport Mechanisms of Nanoparticles Capable of Crossing the BBB.** *5.2.1. Osmotic Agents.* In addition to passive and active transport mechanisms, other forms of BBB manipulations could enhance its permeability, which in turn would increase the possibility of NP crossing. An example of such manipulation is using osmotic agents such as mannitol, ethanol, and dimethyl sulfoxide (DMSO). These agents could facilitate, increase, and improve the transport of different medicines into the brain tissue. Mannitol, which is used to reduce high intraocular pressure and intracranial hypertension,[118] is an osmotic diuretic and metabolically inert in humans. It is often infused via an intra-arterial route to temporarily manipulate the permeability of the BBB[119] and to enable passage of NPs with their cargos from blood vessel capillaries to the brain parenchyma.[120] It was shown that BBB opening with mannitol resulted in faster and higher accumulation of $^{89}$Zr-bevacizumab deferoxamine, and interestingly, this was observed only in the ipsilateral hemisphere.[121]

*5.2.2. Focused Ultrasound (FUS).* Focused ultrasound (FUS) is a noninvasive technique for targeted and reversible BBB interruption with sub-millimeter accuracy that shows significant potential for improving drug delivery into the brain parenchyma and treatment of CNS diseases.[122] Transcranial FUS is frequently combined with intravenously delivered microbubbles (MBs) to disrupt the BBB membrane physical integrity.[123,124] Briefly, the MBs steadily oscillate in a limited and specific area within an acoustic field to create mechanical shear forces and circumferential stresses on the BBB microvasculature walls.[125,126] This would transiently open the BBB in a spatially targeted manner, though the entire structural integrity of the BBB will be restored within 4−6 h after the treatment.[127] In a recent phase I clinical trial, Gasca-Salas et al. (NCT03608553) investigated the efficacy of MR-guided focused ultrasound combined with intravenous microbubbles for temporarily opening the BBB in patients with Parkinson's disease and dementia. The treatments successfully achieved BBB opening in the parieto-occipito-temporal junction in 8 out of 10 treatments across 5 patients, as evidenced by gadolinium enhancement on MRI.[128] Furthermore, the MRI results revealed BBB closure in the putamen shortly after treatment. Importantly, no hemorrhagic or infarct lesions were detected.[129] These promising findings demonstrate the safety and effectiveness of combining focused ultrasound with microbubbles for temporary BBB opening.

*5.2.3. Laser.* Laser stimulation has also been investigated to increase BBB paracellular diffusion of NPs by enhancing permeability through the TJs.[130,131] The local bioeffects generated by the interactions between NPs and picosecond-laser pulses induce a temporary BBB permeability and a higher payload accumulation via diffusion through the paracellular tight junction. Li et al.[130] labeled blood vessels with lectins and then perfused animals to remove excess liposomes from the blood vessels and demonstrated that the BBB manipulation via laser allows antibodies, genes, and liposomes to penetrate the brain parenchyma. This practically presented a valuable, safe, and effective medicinal delivery method in the CNS.[130]

*5.2.4. Magnetic Field Force.* Magnetic nanoparticles (MNPs) are composed of a magnetic iron oxide core and biocompatible surface (e.g., dextran, lipids, polymers, or small molecules). The core is most often magnetite ($Fe_3O_4$) or maghemite ($\alpha$- or $\gamma$-$Fe_2O_3$) with sizes of 1−100 nm.[132] They have been used in drug delivery to the brain. Studies with magnetic NPs are mainly established based on the following three mechanisms: (1) modification with functional ligands, (2) application of an external magnet field (EMF), and (3) use of a low radiofrequency field. The first strategy is similar to RMT, which utilizes peptides, antibodies, and small molecules as NP-attached ligands to facilitate their transport to the brain. The second strategy is to use external magnet force to move MNPs where they can be directed from the blood vessel lumen to the brain parenchyma.[133,134] Magnetic forces can temporarily disrupt endothelial cell−cell junctions through internalized MNPs, activating the paracellular transport pathway and facilitating the local extravasation of circulating substances.[135] The penetration efficiency is closely related to MNP properties (size, magnetic properties, coating, functionalization, and biocompatibility) and external factors (the strength, gradient, and geometry of the magnetic field, the blood viscosity, and flux velocity).[136] Chen et al. found that a static magnetic field assisted MNP penetration through the BBB, increasing it to 8.47% compared to 3.36% without magnetic field treatment.[137] Gupta et al. found that MNPs could penetrate the BBB through the transient disruption of ZO-1, an indicator of BBB integrity. ZO-1 expression was reduced 1 h after magnetic field exposure, partially recovered at 2 h, and reached comparable levels to normal at 3 h. These results validate that MNPs can transiently open TJs to cross the BBB through magnetic hyperthermia induced by the magnetic field. The combination of an alternating magnetic field and an external static magnetic field enhanced MNP crossing to ∼63%, compared to ∼50% with just the external static magnetic field alone. Besides, more MNP accumulation in the mouse brain was observed when applying an alternating magnetic field, demonstrating its ability to modulate BBB permeability through the magnetic guidance of NPs.[138] Gkountas et al.[139] demonstrated that an EMF could significantly enhance MNP delivery across the BBB. Without EMF exposure, 100 nm MNPs showed minimal BBB penetration (2−6%). However, under an EMF intensity of 0.39 T, the BBB crossing efficiency of 100 nm MNPs markedly rose to 40%. Meanwhile, the percentage of 10 nm MNPs passing the BBB was unchanged (<1% difference) with or without EMF. In contrast, the permeability of larger 100 nm MNPs improved by up to 30% under EMF conditions. Maximum permeation of ∼45% was attained using an EMF intensity of 1 T, compared to 42.5% at 0.8 T, 37.5% at 0.5 T, and only 12.5% without EMF. Furthermore, manipulating fluid flow velocity also impacted MNP transcytosis. At a baseline


https://doi.org/10.1021/acsnano.3c10674
ACS Nano 2024, 18, 1820−1845

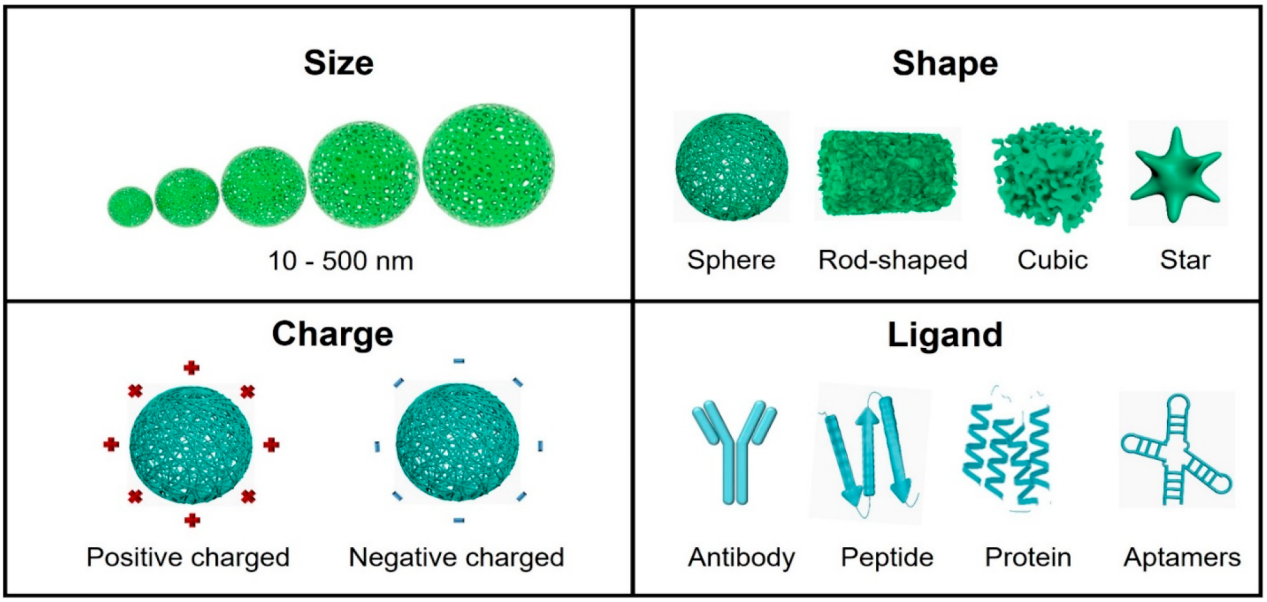


**Figure 6. Overview of nanoparticles developed for the purpose of BBB penetration and their tunable parameters: size, shape, charge, and ligand.**

flow of $10^{-3}$ m/s, the percentage of NPs passing the BBB reached 45%, decreasing to 32% under slow flow ($5 \times 10^{-4}$ m/s) but improving slightly to 48% with faster flow ($2 \times 10^{-3}$ m/s). This demonstrates that EMF intensity and fluid dynamics modulate MNP delivery across the BBB, providing insights into enhancing brain nanoparticle permeation via magnetic guidance.[139] The third strategy is to utilize the heat produced by Néel relaxation of magnetic NPs under the radiofrequency field, which can also transiently and locally open the BBB.[2,140]

*5.2.5. Cell-Mediated Transcytosis.* Cell-mediated transcytosis is a typical method for immune cells to cross the BBB. Different blood-borne immune cell populations, including leukocytes, monocytes, and macrophages, undergo diapedesis and cross the barrier via both paracellular and transcellular routes.[141] This happens in the case of both autoimmune reaction and infection of the CNS.[142] These cells cross the BBB, where there is an increased expression of adhesion molecules on the ECs. The discovery of this mechanism has explored for delivering therapeutic materials to the CNS and an example is the treatment of glioblastoma (GBM). Recently, Li et al. (2021) demonstrated that encapsulating NPs within neutrophils could significantly enhance drug delivery across the BBB *in vitro* and *in vivo*. They found that the penetration rate of the drug-loaded NPs across the barrier increased from 5.2% without encapsulation to 35.6% when enveloped within neutrophils. This effect was mediated by inflammation from GBM, which served to activate and attract the NP-containing neutrophils. In mice with glioblastoma, intravenous injection of the neutrophil-encapsulated NPs led to their accumulation in the brain tumor, with NP levels remaining significantly elevated for 48 h postinjection. This neutrophil "Trojan horse" approach could provide an effective cell-mediated transcytosis strategy to enhance NP drug delivery across the BBB for therapy.[143]

Various strategies have been employed to enable NP penetration across the BBB, including osmotic disruption, focused ultrasound, laser, magnetic guidance, and cell-mediated transcytosis. The former four techniques work primarily through the temporary disruption of TJs between brain ECs. In contrast, cell-mediated transcytosis takes advantage of innate immune cell trafficking pathways that are activated during neuroinflammation and in brain tumors like glioma. While showing promise in enhancing NP delivery to the brain, these strategies need to be further optimized to provide greater permeation while minimizing adverse effects like toxicity, damage to brain vasculature, and loss of BBB integrity.

## 6. PROPERTIES AFFECTING NANOPARTICLE CROSSING THROUGH THE BBB

Different strategies have been employed to improve the BBB penetration proficiency of NPs. Among various approaches,[145−148] a common way is to regulate the Wnt/$\beta$-catenin signaling produced by glial cells and reduce their binding to multiprotein receptor complexes on brain ECs[23] for cargo administration with high BBB penetration potential. The main limitation of all these methods, however, could be the structural damage and, hence, the dysfunction of the BBB.

Another effective strategy to improve the BBB penetration proficiency of NPs is to synthesize the NPs in such a manner that they could actively cross the BBB themselves. Here, we discuss the effects of size, shape, surface charge, and surface ligands of NPs on their BBB permeability (Figure 6).

**6.1. Size Effect of Nanoparticles.** Size effect is an essential factor that needs to be considered when designing NPs because it will directly affect their uptake and permeability through the BBB. NPs of different sizes show diverse circulation half-life time, vascular permeability, and macrophage clearance[149] and have different tendencies to accumulate in different organs. For instance, NPs smaller than 5 nm in diameter could cross the BBB effortlessly. However, their short circulation time and rapid clearance by the kidney will limit their effectiveness and practical applications.[150] NPs in the 5−15 nm size range exhibit broader organ distribution profiles, and particles smaller than 10 nm are prone to renal clearance. In particular, 15 nm NPs have been shown to achieve the highest distribution to the liver, lungs, and kidneys at 24 h postadministration, with additional biodistribution in the


https://doi.org/10.1021/acsnano.3c10674
ACS Nano 2024, 18, 1820−1845

spleen, heart, brain, blood, and stomach. Meanwhile, 20 and 50 nm NPs exhibit maximal accumulation in the liver and spleen at 24 h, distributing additionally to blood, kidneys, heart, lungs, and cerebral cortex.[151,152] On the other hand, NPs in the 50−100 nm size range tend to accumulate nonspecifically in the liver through fenestrations in sinusoidal endothelium.[153,154] At 100−200 nm size, NPs undergo rapid clearance by macrophage phagocytosis in the liver and spleen.[155] NPs at 200−500 nm are inclined to be retained in the spleen.[156] Larger NPs of 2−5 $\mu$m size would accumulate in the pulmonary capillaries[157] and then be cleared by the mononuclear phagocyte system. Obviously, the nanomaterial size, structure, and design are the most critical properties of NPs as carriers for the delivery of cargos across the BBB.

Betzer and colleagues[158] investigated the effect of size on BBB permeability of insulin-coated gold NPs (INS-GNPs) in an *in vivo* model. They synthesized different sized INS-GNPs (20, 50, and 70 nm) and illustrated their distribution by CT and atomic spectroscopy after intravenous (iv) injection. The results showed that the intracerebral concentration of 20 nm INS-GNPs was higher than that of 50 and 70 nm INS-GNPs at 2 and 24 h after iv injection. This could be explained by the fact that the small sized INS-GNPs could cross the BBB easily.[158] Cai et al.[159] chose 2,3-bis(4-(phenyl(4-(1,2,2-triphenylvinyl)phenyl)amino)phenyl)-fumaronitrile (TPET-PAFN) as an aggregation-induced emission fluorogen, which was encapsulated with PEG to form NPs of different sizes (10, 30, 60 nm). In their investigation, NPs of most sizes were unable to cross the intact BBB, but the NPs with smaller sizes (10 and 30 nm) were able to penetrate an altered BBB (induced by photothrombotic ischemia (PTI)).[159] Although most of the NPs display size-dependent BBB permeability, obviously, this is not an absolute rule. Nowak et al.[160] tested the BBB permeability of carboxylated polystyrene (PS) particles of different sizes (100, 200, and 500 nm) in an *in vitro* model. Their BBB replica model was established by immortalized human brain microvascular endothelial cells (hCMEC/D3). The PS particles at 200 nm showed better BBB penetration than the others (10-fold higher than 100 nm and 100-fold higher than 500 nm), indicating a non-monotonic dependence on their properties. This could be explained by the contact areas and the adhesion between NPs and ECs increasing with their size, but the sizes larger than 200 nm tend to accumulate in the kidney and, hence, lead to lower accumulation in the brain.[160]

**6.2. Shape Effect of Nanoparticles.** Shape is another key factor affecting the pharmacokinetics and BBB permeability of the NPs. NPs can be synthesized as spheres, rods, cubes, flat shapes, stars, etc. Their shape will affect their potential for targeting as well as BBB penetration due to their differences in contact quality and contact areas with the target cells in the BBB.[161]

Most nanocarriers are designed to be spherical because of their ease of manufacturing. Nevertheless, this has limited their biological properties, circulation time, targeting potential, and BBB penetration, because of their relatively lower contact areas.[154] Da Silva-Candal and co-workers[162] studied the binding affinity to the cerebral microvasculature cells of polystyrene NPs in diverse shapes (spherical and rod-shaped), in order to evaluate the effect of NP shape on BBB permeability. The binding ability of polystyrene NPs with cerebral microvasculature cells was tested in static (cell culture dishes coated with bEnd.3 cells) and dynamic (flow in microfluidic channels lined with hCMEC/D3 cells) conditions. The rod-shaped polystyrene NPs showed stronger binding ability (2.5-fold increase in static, 1.5-fold increase in dynamic) with cerebral microvasculature cells than the spherical NPs *in vitro*, because the contact areas between the rod-shaped NPs and the cells were much larger.[162] Fu et al.[163] found that the cellular endocytosis efficiency of PEGylated upconversion nanoparticles (UCNPs) was closely related to particle shape, as defined by various aspect ratios (length/width). UCNPs with an aspect ratio of 2 exhibited the highest uptake (86.8%) in hCMEC/D3 endothelial cells, compared to aspect ratios of 1 (spherical, 47.4% uptake), 3 (rod-shaped, 55.9% uptake), or 4 (rod-shaped, 37.6% uptake). UCNPs with aspect ratios of 3 or 4 displayed substantial aggregation and accumulation on cell surfaces, and lower uptake efficiency. In contrast, UCNPs with an aspect ratio of 2 showed good dispersibility and high accumulation in the brain of living zebrafish compared to UCNPs of other aspect ratios. Following UCNP injection in zebrafish, confocal microscopy with 980 nm laser excitation at 2 h postinjection revealed poor dispersion of UCNPs with high aspect ratios (3 or 4) from the injection site, correlating with the aggregation observed in cell cultures. In comparison, PEG-UCNPs with an aspect ratio of 2 exhibited diffusion from the injection site into the zebrafish brain. PEG-UCNPs with an aspect ratio of 1 also showed some diffusion into the brain, although less than those with aspect ratio 2. The brain uptake efficiency of aspect ratio 1 UCNPs was 33.5 ± 4.8% of that for aspect ratio 2. UCNPs with aspect ratio 3 had approximately half the brain uptake of those with aspect ratio 1, while those with aspect ratio 4 had the lowest uptake in the zebrafish brain (only 8.7 ± 0.6% of those with aspect ratio 2).[163] Undoubtedly, the paradigm regarding NPs with different morphologies is of great significance to the delivery design concept in bio-nanotechnology tools and their application in nanomedicines.

**6.3. Surface Charge Effect of Nanoparticles.** The charge on the surface of polymeric NPs affects their properties, like circulation life, BBB permeability, cytotoxicity, and so on. Positively charged particles can effectively target tumor blood vessels, and neutrally charged particles show faster diffusion.[164] Neutrally and positively charged NPs show lower serum protein adsorption in blood circulation, thus manifesting a longer circulating time than negatively charged NPs.[165] Brain EC membranes contain relatively more negatively charged phosphatidylserine and phosphatidylinositol and exhibit higher negative charges than other EC vasculars. The high negative charge not only provides an additional protective barrier for the brain but also regulates the entry of macromolecules and other charged cargos, like drugs or carriers such as NPs, into the CNS.[166] Cationic NPs can be adsorbed to the plasma membrane surface of the EC through electrostatic interaction and then cross the BBB by adsorptive-mediated endocytosis, thus, exhibiting higher BBB permeability.[167] However, compared to neutral and negatively charged NPs, cationic NPs showed higher cytotoxicity to ECs, and high macrophage uptake and clearance.[168] Therefore, it is important to consider the benefit-to-risk ratio and adjust the surface charge of NPs to make them highly penetrable to the BBB with low cytotoxicity. Zhang et al. investigated the BBB penetration of two different charged (neutral and positive) polystyrene nanospheres in an *in vitro* BBB model. Their results indicated that the positively charged NPs exhibited significantly higher BBB penetration capacity than the neutral molecules by approximately 100-


https://doi.org/10.1021/acsnano.3c10674
ACS Nano 2024, 18, 1820−1845

fold.[169] Chen et al.[170] have demonstrated that the surface charge of mesoporous silica nanoparticles (MSNs) plays a critical role in their ability to cross the BBB in zebrafish models. Specifically, 50 nm MSNs with a highly negative surface charge (zeta potential of approximately −40 mV) achieved significant accumulation in the brain parenchyma of zebrafish embryos, superior to MSNs with lesser negative charge. In contrast, positively charged MSNs (+18.1 mV and +42.3 mV) showed very limited brain penetrance, indicating enhanced BBB crossing by negatively charged particles. Analysis of the NP protein corona revealed enrichment of three known BBB transporter proteins, afamin, apolipoprotein E, and basigin, on the highly anionic MSNs, providing a mechanistic rationale for their enhanced BBB penetrance compared to cationic and lower charged MSNs. Fluorescence microscopy of larval zebrafish brains demonstrated striking accumulation of N4-RMSN50@PEG/THPMP, a highly negative MSN variant, outside of blood vessels, reflecting extensive parenchymal diffusion. Far fewer cationic MSNs (P1- and P4-RMSN50@PEG/TMAC) or weakly negative particles (N1-RMSN50@PEG) crossed the BBB. High resolution two-photon microscopy and histological analysis corroborated and extended these findings, clearly delineating accumulation of N4-RMSN50@PEG/THPMP within the brain. Taken together, these results demonstrate that a highly negative nanoparticle surface charge promotes BBB transport likely by enrichment of protein corona components that engage endogenous BBB transport mechanisms. Modulation of surface charge could enhance the delivery of nanomedicines across the BBB and into the central nervous system.[170]

**6.4. Surface Ligand Effect on Nanoparticles.** In order to enhance the BBB permeability of NPs by receptor-mediated transcytosis (RMT), numerous promising targeting ligands such as plasma proteins, antibodies, peptides, and aptamers have been reported. For instance, transferrin (Tf) is ferritin that can cross the BBB by binding to the transferrin receptor (TfR) on the surface of ECs and has been widely used in the modification of nanocarriers as brain-targeting ligands.[171] Kuo et al. developed solid lipid NPs grafted with Tf and folic acid (FA) to deliver genes (BV6 and GDC0152) into the brain for the treatment of GBM multiform. Such modification with the Tf could prolong the circulation time of the NPs by avoiding their direct contact with plasma proteins. Additionally, the BBB permeability was favored by Tf binding with the Tf receptor and FA receptor through RMT.[172] Apolipoprotein E (ApoE) is a fat-binding protein, showing a high affinity to the low-density lipoprotein receptor (LDLR) and some low-density lipoprotein-associated receptors (LRPs). ApoE has been widely used for the functionalization of polymeric NPs to elevate their BBB permeability.[173] Zhang et al. (2020) constructed NPs with bovine serum albumin (BSA) coated with a dopamine shell, then linked COG1410 (an apolipoprotein E mimetic peptide that can transport NPs across the BBB) on the surface. This nanoplatform could effectively deliver itraconazole into the brain, and display promising therapeutic effects for meningitis caused by *Candida albicans*.[174] Moreover, platelet-derived growth factor receptor $\beta$ (PDGFR$\beta$) is a kind of tyrosine kinase receptor located on the surface of the cell membrane. Its function mainly is to regulate cell proliferation, differentiation, growth, and development. Monaco et al.[175] developed a nanovector conjugated with the anti-PDGFR$\beta$ aptamer. This nanovector was successfully used to deliver the chemotherapeutic drug NVP-BEZ235 into the brain and target the PDGFR$\beta$ overexpressed on the endothelial cells of vessels. Furthermore, the anti-PDGFR$\beta$ nanovectors accumulated in the brain at 2 and 4 h after systemic administration.[175] Li et al.[176] demonstrated that modification of NPs with the rabies virus glycoprotein peptide (RVG29) enabled effective transport across the BBB in cellular and animal models of Parkinson's disease. In bEnd.3 BBB model cultures, RVG29-functionalized NPs encapsulated in neutrophil-derived membranes (RVG@AHM@Pt/CeO2) exhibited a 2.12-fold enhancement in BBB transit compared to nontargeted particles (AHM@Pt/CeO2). This was accompanied by less retention of RVG-modified NPs (81.33% of that in AHM@Pt/CeO2) in the upper chamber after transit, reflecting excellent BBB penetration performance. Similarly, *in vivo* imaging in Parkinson's mice showed pronounced BBB permeability and brain retention only for RVG29-modified, cell membrane coated NPs. Those NPs lacking RVG29 functionalization remained largely within the circulation. Together, these findings demonstrate that rational modification of cell membrane-coated NPs can achieve targeted delivery across the BBB. The modular RVG29 targeting ligand, derived from a neurotropic virus, binds specifically to receptors at the BBB to trigger transcytosis. Combining cell membrane camouflage and selective BBB targeting ligands is a promising approach to improving central nervous system delivery of NPs for therapy development.[176] Zhang et al.[177] demonstrated a micelle-based drug delivery system that enhanced the transport of antiepileptic drugs (AEDs) across the BBB. The micelles were comprised of ferrocene-conjugated D-$\alpha$-tocopherol poly(ethylene glycol succinate) (TPGS-Fc) and amphiphilic copolymer Poloxamer 407, enabling high encapsulation of diverse AEDs. Key features of the TPGS-Fc micelles, including transferrin receptor binding and P-glycoprotein efflux pump inhibition, promoted BBB penetration. Cellular uptake and BBB transmigration studies in bEnd.3 models verified improved BBB transit of TPGS-Fc micelles loaded with a fluorescent probe compared to free drug. They showed highly enhanced fluorescence intensity (31.5 ± 8.2%), which demonstrated the high efficiency in improving drug penetration of the BBB. BBB transit was decreased from 28.7 ± 3.4% to 18.9 ± 3.1% through pretreatment with transferrin, implicating receptor-mediated transcytosis as the mechanism. ATP assays also revealed that TPGS-Fc micelles inhibit P-glycoprotein, further enhancing brain permeation by averting efflux. *In vivo* imaging in mice showed a 2.4-fold increase in brain accumulation of AEDs loaded in TPGS-Fc micelles compared to free dye at 36 h postinjection. Whole brain imaging and sectioning corroborated micelle-mediated enhancement of brain delivery, 2.4-fold that in the free dye group. In summary, the rational design of TPGS-Fc micelles promoted the delivery of AEDs across the BBB via transferrin receptor binding and P-glycoprotein inhibition. This system shows promise for improved pharmacotherapy of epilepsy and potentially other CNS disorders.[177] In another study, Nong et al.[178] demonstrated that targeting the adhesion molecule ICAM-1 enabled the transport of NPs across the BBB. They intravenously injected NPs conjugated to anti-ICAM-1 antibodies. Initially, a large fraction (>20%) of the anti-ICAM NPs localized to the lungs and associated with pulmonary leukocytes (>90%). Over time of 0.5 h, 4 h, and 22 h, the anti-ICAM NPs and pan-leukocyte marker (CD45) decreased in the lungs and increased up to 5-fold in the brain, suggesting the initial delivery of $\alpha$ICAM to activated leukocytes in the


https://doi.org/10.1021/acsnano.3c10674
ACS Nano 2024, 18, 1820−1845

pulmonary vasculature followed by migration of leukocyte-loaded NPs to the injured brain across the BBB. Intravital microscopy visually confirmed anti-ICAM nanoparticles localized to inflamed brain vasculature after injection. The number of detectable NPs in the brain parenchyma increased over 22 h, indicating the crossing of the BBB. Flow cytometry revealed the nanoparticles in the brain were almost entirely taken up by leukocytes (98.7%). Specifically, 73% of nanoparticle-positive leukocytes were monocytes/macrophages and 24.5% were neutrophils. Histology showed nanoparticles largely colocalized with macrophages in the brain parenchyma. In summary, targeting ICAM-1 enables leukocytes to act as Trojan horses to carry the NPs across the BBB during neuroinflammation.[178]

## 7. FUNCTIONALIZED POLYMERIC NANOMATERIALS CROSSING THE BBB

Many nanomaterials, encompassing poly(ethylene glycol), poly(lactic-*co*-glycolic acid) and other categories, exhibit distinctive physicochemical properties and multifunctional modification, rendering them pivotal carriers for therapeutic agents across the BBB. The exploration of various nanoparticles, including those based on polymers, lipids, and metals, has been a focal point of research over the years, leading to the emergence of noteworthy findings (Table 3).

**Table 3. Summary of Various Polymeric NPs Capable of Crossing the BBB**

| polymer | BBB targeting agents | application | ref |
|---|---|---|---|
| PEG | Pen peptide | AD therapy | 179 |
| PEG | AGBBB015F and Regulon peptides | brain glioma treatment | 180 |
| PEG | lactoferrin | glioblastoma therapy | 181 |
| PEG | lactoferrin | BBB crossing | 182 |
| PEG | $CD4^+$ $T_{EM}$ cells | BBB crossing | 183 |
| PLGA | DBP | AD therapy | 184 |
| PLGA | RVG29 peptide | BBB crossing | 185 |
| PLGA | Angiopep-2 peptide | BBB crossing | 187 |
| PLGA−PEG | RVG29 peptide | PD treatment | 188 |
| liposomes | RVG29 peptide | PD treatment | 189 |
| PEGylated liposomes | transferrin | glioblastoma therapy | 191 |
| lipoprotein | T7 peptide | glioma-targeted therapy | 192 |
| PEI | RGD peptide | glioblastoma therapy | 193 |
| PEI | cRGD peptide | glioblastoma therapy | 194 |
| PEI−PEG | HER2 antibody | malignant glioma treatment | 195 |
| PLA | MPC monomer | BBB crossing | 197 |

**7.1. Poly(ethylene glycol) (PEG)-Modified Nanomaterials.** Poly(ethylene glycol) (PEG) is commonly manufactured by the addition polymerization of ethylene oxide and water or ethylene glycol with the chemical formula $HO-(CH_2CH_2O)_nH$. PEG is widely employed in biomedical applications because of its outstanding biocompatibility in physiological microenvironments. For example, Ru@Pen@PEG-AuNS was constructed by Yin et al.[179] to alleviate AD, in which these NPs specifically acted as nanovehicles with higher BBB permeability potential. In their study, the gold nanostars (AuNSs) were formed via a seed-mediated growth process and served as photothermal agents under 808 nm laser excitation. The biocompatibility and physiological stability of the NPs were also significantly improved through linking with PEG. The surface of PEG-AuNS was also coated with the penetratin (Pen) peptide, a cell-penetrating peptide (CPP) of 16 amino acid residues that has a strong ability for cellular internalization and, hence, BBB crossing. Lastly, the final NPs were tagged with ruthenium (Ru) to obtain the luminescent attribute. The final Ru@Pen@PEG-AuNS NP construct demonstrated a strong neuroprotective benefit and great BBB diffusion in the AD mouse model.[179] In 2018, polyester-based NPs with biodegradable block copolymers were prepared by Borrós et al.[180] through the polycondensation technique. These NPs (i) coated with PEG, (ii) conjugated with BBB-crossing peptides (AGBBB015F and Regulon REG), and (iii) loaded with PTX were effectively employed to treat glioma.[180] Overall, such NPs with high drug loading capacity (by exhibiting a strong binding affinity with low-density lipoprotein receptors) could facilitate crossing of the BBB via receptor-mediated transcytosis. Additionally, Kuo et al. (2016) developed a form of BBB-crossing solid lipid-based nanocarriers (SLNs) designed with tamoxifen (TX) and lactoferrin (Lf) ligands to deliver carmustine (BCNU), which is an anticancer agent and GBM multiforme growth suppressor, into the brain parenchyma.[181] Interestingly, the BCNU-loaded SLNs that have been customized with TX and Lf ligands displayed ten times higher BBB permeability compared to the naked BCNU-loaded SLNs. In this dynamic system, the Lf ligand was exploited to coordinate the transcytosis across the BBB through a receptor-mediated mechanism, and the TX acted as a selective estrogen receptor modulator to compensate for the efflux loss. These NPs have been acknowledged as promising delivery agents for GBM pharmacotherapy with noticeable properties in crossing the BBB.[181] Furthermore, Song and co-workers[182] designed a pharmaceutical brain-delivery system through a microemulsion process to fabricate biocompatible silica NPs and covalently modified them with Lf receptor and PEG. The Lf facilitated BBB targeting by the receptor-mediated transcytosis process. In addition, these NPs could avoid being trapped in the reticuloendothelial system by PEG due to their substantial solubility and long half-life in blood circulation. The size of these specially designed NPs ranged from 25 to 100 nm. Obviously, the smaller size NPs showed higher efficiency in infiltrating and crossing the BBB. It was also reported that such NPs showed promising prospects as brain delivery carriers and brain imaging probes.[182] More recently, Klok et al.[183] developed NP-decorated T cells capable of migrating across the BBB independent of any specific antigen and under static conditions and physiological flow. As shown in Figure 7, they were formed by activating effector/memory $CD4^+$ helper T cells ($CD4^+$ TEM cells) with an approximate diameter of 200 nm and PEG-modified polystyrene NPs using a thiol−maleimide covalent coupling strategy. Besides, the NPs were almost exclusively colocalized with the cell membrane. Noticeably, even the presence of ∼105 NPs per cell did not compromise the ability of the $CD4^+$ TEM cells to bind to the intercellular adhesion molecule-1 (ICAM-1) and cross the BBB, despite the loss of NP cargo during diapedesis in several cases.[183]

**7.2. Poly(lactic-*co*-glycolic acid)-Modified Nanomaterials.** Poly(lactic-*co*-glycolic acid) (PLGA) is randomly polymerized and composed of two monomers, lactic acid and glycolic acid. PLGA is biodegradable, biocompatible, and nontoxic, and because of that, PLGA is widely used in pharmaceutical products and other industries. Hence, the


https://doi.org/10.1021/acsnano.3c10674
ACS Nano 2024, 18, 1820−1845

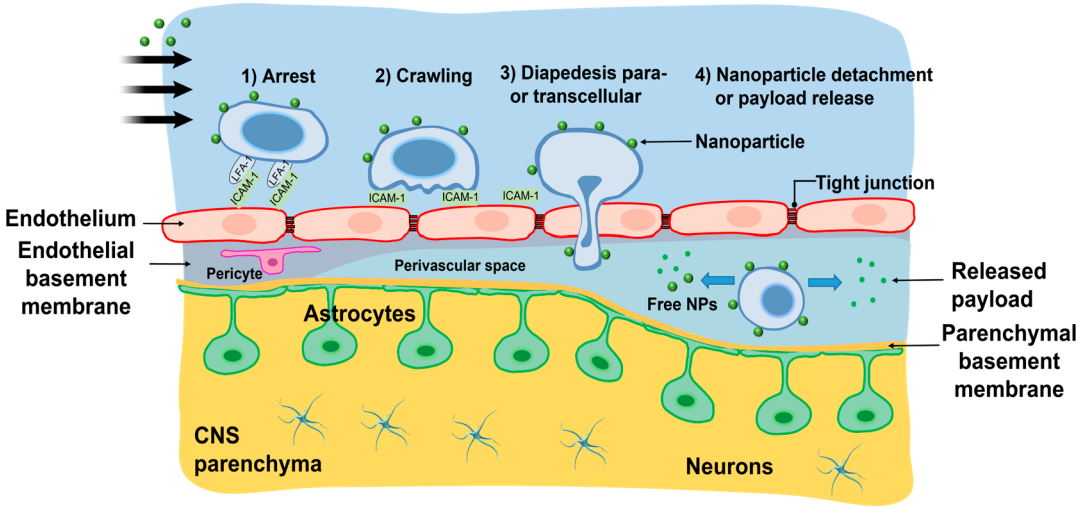


**Figure 7. Schematic diagram of NP transport over the BBB via CD4$^+$ TEM cells. After reaching the CNS parenchyma, the NPs first attach to the myeloid cells and penetrate the BBB endothelium before detaching themselves and releasing their cargos. Reproduced with permission under a Creative Commons License from ref 183. Copyright 2021 the Authors, published by Wiley-VCH GmbH).**

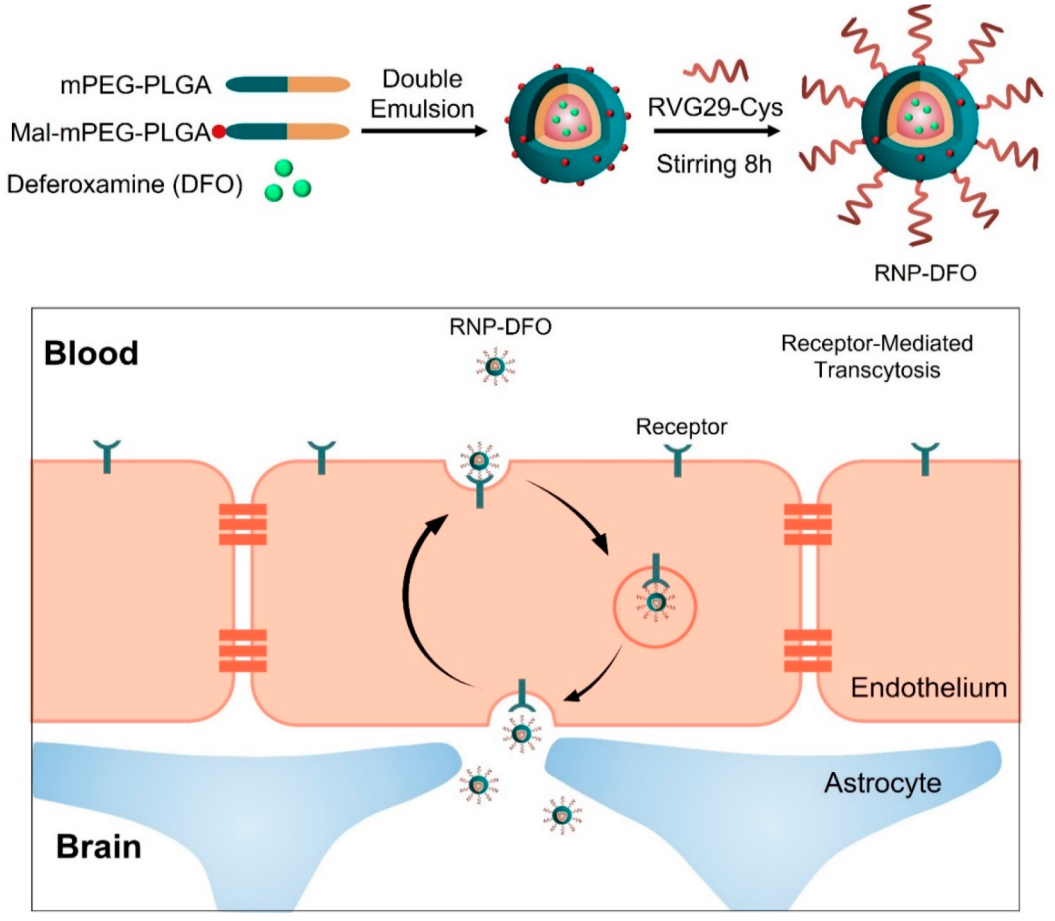


**Figure 8. Schematic diagram of the synthesis of RNP-DFO and the proposed mechanism of their penetration into and crossing of the BBB. The brain endothelial cells are bounded by cell surface receptors along with the RVG29 peptide, which facilitates transcytosis of NPs. Reproduced with permission from ref 188. Copyright 2018 American Chemical Society).**

exciting properties of PLGA in crossing the BBB were extensively investigated. In 2019, Jeon et al. designed functionalized PLGA NPs, coupled with the vitamin D-binding protein (DBP) through an emulsion diffusion approach, and successfully tested them in AD treatment *in vitro*.[184] It is known that DBP can greatly reduce amyloid beta (A$\beta$) peptide aggregation, which is one of the predominant causes of AD. As a result, DBP-PLGA NPs exhibited a better therapeutic effect to impede A$\beta$-polymerization than the free DBP at the same dose for AD therapy. The DBP-PLGA NPs presented an


https://doi.org/10.1021/acsnano.3c10674
ACS Nano 2024, 18, 1820−1845

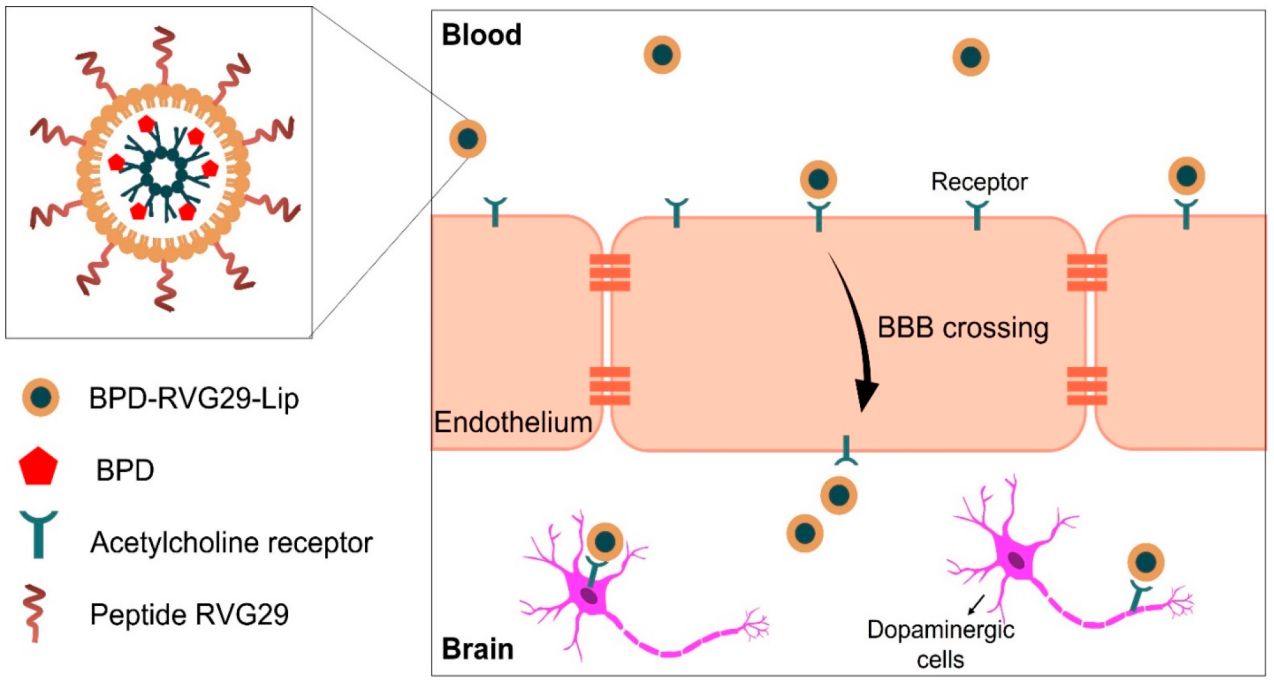


**Figure 9. Schematic illustration of RVG29 modified PEGylated liposomes for crossing the BBB and achieving targeted therapy in a PD model. Reproduced with permission from ref 189. Copyright 2018 Elsevier.**

effective platform for delivering cargo to the CNS due to their impressive abilities in crossing the BBB. In another study, the dendrimer poly(amidoamine) (PAMAM) was conjugated with bovine serum albumin (BSA) by carboxyl activation to develop dendrimer-cationized-albumin (dCatAlb), which was subsequently linked with doxorubicin (DOX)-loaded PLGA NPs to form dCatAlb-pDNP NPs. In this study, the caveolae- and clathrin-mediated process through either endocytosis or absorptive-induced transcytosis was reported to be responsible for the internalization of the NPs. They displayed better BBB penetration via absorptive-induced transcytosis due to the cationic attribute of the BSA and therefore were positively tested to treat glioblastoma successfully.[184] Recently, Chung et al.[185] synthesized a biodegradable and biocompatible form of PLGA NPs to be employed for CNS drug delivery. A 29-amino-acid rabies virus glycoprotein (RVG29) was capped on the surface of PLGA, enabling these polymeric NPs to cross the BBB by targeting the nicotinic acetylcholine receptors. And because of such surface modification, the blood residence time of these PLGA NPs was extended, and consequently, the exposure of cargo to the BBB was enhanced too. The RVG29 receptors facilitated the intranasal delivery of RVG29-capped NPs to the brain with quick kinetics.[185] Cano et al.[186] developed PEGylated PLGA via a double emulsion approach to "envelop" epigallocatechin-3-gallate (EGCG) and ascorbic acid (AA) for AD therapy. These functionalized NPs had optimum bioavailability and when they were injected intraperitoneally in the mice model of AD, showed significant therapeutic efficacy by enhancing spatial learning and improving memory in the AD mouse model. This presented a safe and effective strategy to increase synaptophysin expression and decrease neuroinflammation in the nervous system.[186]

Tosi et al.[187] constructed functionalized PLGA-NPs with angiopep-2 (Ang-2) through the nanoprecipitation approach. Ang-2 is a BBB penetrating peptide, which can bind with the low-density lipoprotein receptor-related protein 1 (LRP1) in the CNS. These NPs displayed the potential tp accumulate in the brain and, hence, presented a promising tool for targeted nanomedicines (Ang-2) in AD. Furthermore, these NPs could be employed as cargo-carriers for delivering various pharmaceutical agents into the CNS parenchyma, therefore significantly expanding the therapeutic possibilities.[187] In another case, Nie et al. developed an RVG29 peptide-conjugated monomethoxy-PEG (mPEG)-PLGA NP (RNP-DFO) that enabled DFO (an iron chelation drug approved by the FDA for refractory anemia) to circulate for a longer period of time, while also being effectively delivered to the brain.[188] This demonstrated a specific affinity between the RVG29 peptide and its receptors on the brain's microvascular endothelium, facilitating the BBB crossing of the NPs into neurons. The delivered cargo (drug) would eliminate surplus cellular iron, triggering the decrease in iron-related oxidative stress resulting from the delivery of the iron chelator DFO across the BBB (Figure 8). Besides, no *in vivo* neuronal apoptosis or other nontargeted adverse effects mediated via NPs were observed. Such a strategy of administering iron chelators for PD treatment could in turn be employed to safely and effectively distribute DFO in the brain.

**7.3. Lipid-Based Nanocarriers.** Lipids are organic compounds very suitable for acting as a nanocarrier to penetrate the BBB and deliver cargo. Qu et al.[189] developed therapeutic PEGylated liposomes, which were modified with RVG29 peptide through the maleimide and thiol coupling reaction and loaded with *N*-3,4-bis(pivaloyloxy)-dopamine (BPD). The results confirmed the efficiency of RVG29-modified PEGylated liposomes (RVG29-lip) in crossing the BBB, which was much higher than the PEG-liposomes (Figure 9). This strategy was also implemented to achieve targeted therapy in the PD mouse model.[189] Rehman et al.[190] created a brain therapeutic delivery system based on thermoresponsive lipid NPs (TLNs) using the hot melt encapsulation approach.


https://doi.org/10.1021/acsnano.3c10674
ACS Nano 2024, 18, 1820−1845

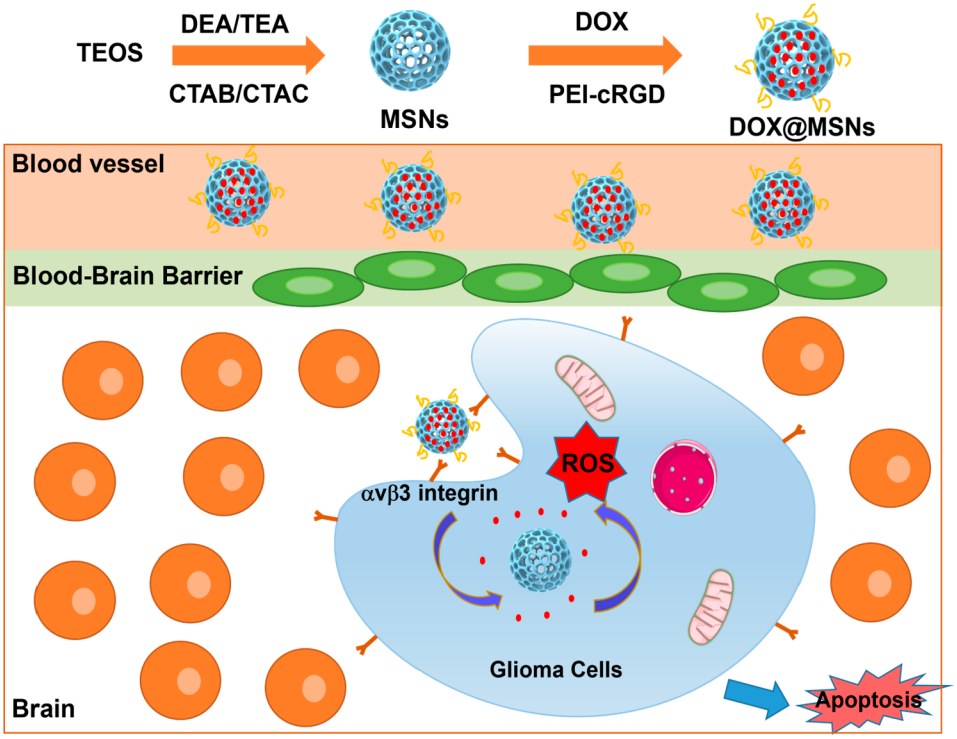


**Figure 10. Schematic illustration of MSN NPs enhancing BBB permeability and antiglioma effect. Reproduced with permission from ref 194. Copyright 2016 American Chemical Society.**

The NPs were packed with paclitaxel (PTX) and employed as a nanocarrier, which was able to infiltrate the BBB and then target glioblastoma cells. These lipid NPs are in the solid state at 37 °C and convert to a liquid state at 39 °C (solid−liquid transition). For this reason, the liquid state could easily be distorted and squeezed past the BBB tight connections. The rapid diffusion of pharmaceuticals from liquid NPs successfully resulted in quicker drug release.[190] The high permeability and BBB delivery of TLNs were demonstrated via an *in vitro* model achieving the three main elements in CNS drug delivery, BBB crossing, rapid diffusion of the carrier, and fast release of cargo. Jhaveri et al.[191] developed and reported *in vitro* and *in vivo* investigations using transferrin-targeted liposomes for delivering resveratrol (RSV) to treat GBM. The liposomes were produced via the thin film hydration method, and RSV was loaded into them to synthesize RSV-laden PEGylated liposomes (RSV-L) with the goal of improving the physiochemical characteristics of RSV. The RSV-L NPs with high encapsulation efficiency and a lengthy drug release period were subsequently bonded to transferrin moieties at the end of the liposome chains (Tf-RSV-L) in order to make them "cancer cell specific". Distinctly, the Tf-RSV-L NPs crossed the BBB by exploiting transferrin as a receptor via receptor-mediated endocytosis.[191] In addition, Liang et al.[192] reported a dual-targeting delivery system T7-LDL, which was comprised of low-density lipoprotein particles (LDL) modified with the T7 peptide, a seven-peptide transferrin ligand (TfR). Since the T7 peptide is capable of binding to transferrin receptors on both the BBB and glioma cells and LDL can specifically interact with LDL receptors on brain endothelial cells, the presence of TfR and LDL together could greatly facilitate BBB penetration via receptor-mediated transcytosis. In a follow-up study, the pharmaceutical vincristine sulfate (VCR) was incorporated in the T7-LDL composite by direct hydration of the lipid film and then effectively employed for glioma treatment in both *in vitro* and *in vivo* models.[192]

**7.4. Polyethylenimine-Modified Nanomaterials.** Polyethylenimine (PEI) is a water-soluble polymer, which could act as a cross-linking agent in various bioapplications. You et al.[193] developed an RGD (arginine-glycine-aspartate) peptide-modified mesoporous silica-based nanocarrier for delivering benzo[1,2,5]selenadiazole-5-carboxylic acid (BSeC) to the brain for glioma treatment. Because of the presence of RGD in the structure of these nanomaterials, which behaves as an agent to bind to $\alpha_v\beta_3$ integrin receptors overexpressed on BBB endothelial cells, their BBB permeability was enhanced. The BSeC@MSNs-RGD with PEI coating was found to cross the BBB and disrupt brain cancer U87 VM channels and displayed inhibitory effects on the U87 tumor, therefore validating its anticancer efficacy *in vivo*.[193] In another example, Chen et al.[194] developed DOX@MSNs and showed that these NPs were able to penetrate the BBB, target tumor tissues, and contribute to much higher antiglioma efficacy. The sizes of the mesoporous silica nanoparticles (MSNs) were tailored by modulating the hydrolysis rate and polycondensation degree of reactants, with (i) CTAB/CTAC as the template, (ii) TEOS as the silica source, and (iii) DEA/TEA as the base catalyst. The cancer-targeting efficiency of the NPs was enhanced by conjugation with cRGD peptide, which specifically recognizes and binds to U87 cells with a greater expression level of $\alpha_v\beta_3$ integrin. Further, antineoplastic DOX (doxorubicin) was loaded into the NPs to inhibit glioma cell growth as well. DOX@MSNs could rapidly enter the cancer cells, resulting in higher drug accumulation in the cytoplasm (Figure 10). DOX@MSNs evoked glioma cell apoptosis through inducing ROS overproduction. DOX@MSNs (~40 nm) had high permeability across the BBB and disrupted the vasculogenic mimicry of glioma cells by the downregulation of E-cadherin,


https://doi.org/10.1021/acsnano.3c10674
ACS Nano 2024, 18, 1820−1845

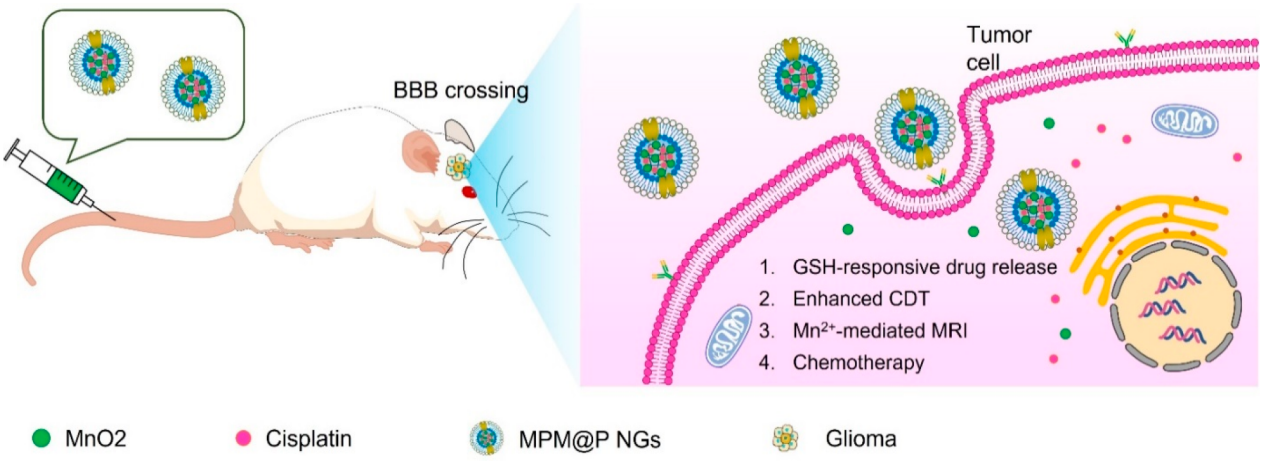


**Figure 11. Schematic diagram of the multifunctional polymer nanogels for BBB crossing, MR imaging, and chemotherapy of orthotopic glioma. Reproduced with permission from ref 198. Copyright 2021 American Chemical Society.**

FAK, and MMP-2 expression. Ideally, this could result in better antiglioma activity with less side effects and toxicities to the surrounding healthy cerebral tissue.[194] In 2018, Chen et al.[195] designed HER2@NPs capable of crossing the BBB and efficiently delivering anticancer agents into the brain tissues. The HER2@NPs were constructed using selenium NPs with surface modification of HER2 antibody, which has a higher binding affinity to its receptors overexpressed in glioma cells. HER2@NPs can efficiently deliver both therapeutic (Cu-phen) and diagnostic agents (superparamagnetic iron oxide NPs) across the BBB to the tumor tissues and enhance their impact on brain cancer therapy and magnetic resonance imaging. In this case, Cu-phen is consistently linked to Cu@HER2@NPs when circulating in the blood and could be rapidly released after lysosome escape. From a mechanistic point of view, Cu@HER2@NPs limit the growth, migration, and invasion of U251 glioblastoma via HER2 receptor-mediated endocytosis and trigger DNA damage-mediated p53 signaling pathways. Moreover, Cu@HER2@NPs could cause apoptosis in U251 cells by increasing ROS.[195]

**7.5. Other Polymeric Nanomaterials.** Recently, some other drug-related NP constructs were explored and widely utilized for diagnostics and therapeutics. Aguilera et al.[196] reported magnetic iron oxide NPs, which were coated with carboxymethyl cellulose (CMC) to form $Fe_3O_4$@CMC via electrostatic interaction. These NPs were potential candidates for brain treatment after conjugation with dopamine hydrochloride. They demonstrated that CMC-modified magnetic NPs are able to traverse human lung microvascular endothelial (HLMVE) cells through endocytosis, which was employed as a BBB model.[196] Furthermore, bioinspired NPs were constructed by Lu et al.[197] that could effectively cross the BBB and deliver medicine to the CNS. The NPs were formed by a core protein and a thin shell polymerized by 2-methacryloyloxyethyl phosphorylcholine (MPC) monomer and poly(lactide)-*b*-poly(ethylene glycol)-*b*-poly(lactide)-diacrylate triblock copolymer (PLA-based cross-linker). The MPC comprises a choline and acetylcholine analogue, which interacts with nicotinic acetylcholine receptors (nAChRs) and choline transporters (ChTs). The MPC could be actively transported from the bloodstream to the brain via energy-dependent transcytosis. After permeating the BBB, the cross-linker is cleaved, the nanocapsule shells are broken down, and subsequently, the active protein payloads are released into brain tissues.[197] Shi et al.[198] utilized the reduction-responsive poly(*N*-vinyl caprolactam) nanogel (PVCL NG) as a carrier. Stable particles (106.3 nm) of colloidal NGs were synthesized by loading $MnO_2$ and the chemotherapeutic drug cisplatin. Subsequently, the macrophage membrane was externally coated, and the macrophage membrane-based biomimetic multifunctional responsive drug-carrying nanogel (MPM@P NGs) was developed (Figure 11). This enabled them to efficaciously achieve the combined treatment of *in situ* glioma with real-time MR imaging monitoring. The functionalized nanogels were able to block the function of targeted glioma and cross the BBB, exploiting the interaction between macrophage membrane-specific proteins (such as integrin $\alpha_4$, $\beta_1$, etc.) and vascular cell adhesion molecule-1 (VCAM-1) at the tumor site. In addition, the *N*,*N*′-bis(acryloyl) cysteamine (BAC) cross-linked PVCL nanogels containing disulfide bonds showed a desirable reduction response to high concentrations of GSH (10 mM) in tumor cells. GSH can break the disulfide bond and disintegrate the nanogels, thus the drug release at tumor sites can precisely be controlled.[198]

In another study, RSV was used for the treatment of oxidative stress induced by excess reactive oxygen species, which is one of the predominant causes of neurological diseases in the CNS. Cui et al.[199] loaded MSNs with RSV and utilized them as drug delivery nanocarriers after being capped with poly(lactic acid) (PLA) as a gate keeper. They were also modified with low-density lipoprotein receptors (LDLR) as ligand peptides through covalent bonding with PLA. The PLA enables the manipulation of the pharmaceutical release-times due to its biodegradable property. The LDLR peptides facilitated the transcytosis process of MSNs to permeate the BBB via receptor-mediated transcytosis, as evidenced by an *in vitro* BBB model (established by rat brain microvascular endothelial cells and microglia cells using Transwell chambers).[199] Additionally, Tang et al.[200] synthesized NK@AIEdots with superior BBB permeability and excellent ability to inhibit glioma growth. The NK@AIEdots were prepared through wrapping a natural killer cell membrane over an aggregation-induced emission (AIE)-active polymeric nanoendoskeleton (AIEdots) PBPTV, which worked as a photothermal agent under 808 nm laser excitation. The NK@AIEdots exhibited an exceptional NIR-II brightness (quantum


https://doi.org/10.1021/acsnano.3c10674
ACS Nano 2024, 18, 1820−1845

yield ≈ 7.9% in water), outstanding stability, excellent biocompatibility, and low cytotoxicity. The surface of NK@AIEdots accurately conserved the complexity of the NK membrane (similar to integrin LFA-1 and VLA-4). They could disrupt tight junctions and reorganize actin cytoskeleton to enhance their abilities to cross the BBB. Besides, NK@AIEdots can specifically accumulate in the brain tumors via DNAM-1/NKG2D receptors and inhibit tumor growth greatly via localized hyperthermia induced by NIR light irradiation. Therefore, these NK-cell-mimetic nanorobots proved to be rather effective BBB-crossing drug delivery agents for the treatment of various neuropathologies.[200]

## 8. CHALLENGES, DIRECTIONS, AND FUTURE PERSPECTIVES

Although functionalized nanomaterials have exhibited exceptional neurotheranostic prospects because of their desired properties of crossing the BBB, still their safety and efficacy make their clinical translation from bench to bed side challenging. Previous studies have extensively revealed the cytotoxicity, genotoxicity, and immunotoxicity of diverse nanomaterials and demonstrated that their toxicity is related to their attributes, numbers, coatings, shapes, sizes, surface charges, surface areas, core structures, surface modifications, and exposed cell types. Another challenge in this field is understanding of the BBB structural and physiological properties, especially when they are compromised during a pathological event, like tumor growth or chronic diseases. The tight junctions between endothelial cells in the BBB restrict the passage of molecules, including therapeutic agents, into the brain. Additionally, the presence of efflux transporters further hinders drug delivery. Therefore, developing functionalized nanomaterials that can effectively bypass or overcome these barriers should be one of the practical aims. Another one is the absence of targeted delivery. Achieving targeted delivery of functionalized nanomaterials to specific brain regions remains a challenge. The complexity of the compromised anatomy and physiology of the brain (due to the ongoing pathologies) and its diverse cell types make it difficult to achieve precise targeting.

Based on these, the potential research directions could be focused as follows: (1) Advanced nanomaterial design: Developing functionalized nanomaterials with improved properties, such as enhanced stability, biocompatibility, and BBB permeability, is a promising direction. This includes the use of advanced nanomaterials, such as carbon-based nanomaterials, liposomes, or polymeric nanoparticles. (2) Conjugation strategies: combining functionalized nanomaterials with other approaches, such as drug delivery systems or imaging agents, can improve their efficacy and enable multifunctionality. Coating nanomaterials with targeting ligands or encapsulating therapeutic agents within nanocarriers can enhance BBB crossing and targeted delivery. (3) developing noninvasive methods for delivering functionalized nanomaterials across the BBB is an emerging direction. Techniques such as focused ultrasound, magnetic targeting, or intranasal delivery offer potential noninvasive strategies for enhancing BBB permeability.

Furthermore, it is undeniable that multifunctional nanomaterials as well as various form of nanodelivery platforms will be important paths for the future progress in prevention, diagnostics, therapeutics, and prognostics.[201] Among numerous strategies, one is a multidisciplinary path to create multifunctional nanosystems that (i) are responsive to the cellular microenvironment, (ii) are capable of safely crossing the BBB and reaching the neuronal parenchyma, (iii) are capable of precisely targeting the cell and tissues of interest, (iv) have optimum capabilities for safe drug delivery, (v) allow effective drug release, and (vi) have acceptable minimum side effects. Certainly, imaging modalities, like MR imaging, positron emission tomography imaging, and optical and photoacoustic imaging could also be employed to develop, boost, and expand such systems. For instance, upconversion nanoparticles (UCNPs) have a wide range of biological applications[168,201−223] and could be introduced for tracking and coupling polymer luminescent research. Future investigations could take advantage of the unique characteristics of the nanomaterials for combining diagnosis and therapies by creating and integrating various functional groups within one nanosystem to achieve highly sensitive and specific tasks. Imaging-guided targeted therapy is one outstanding example, though it is still in the early stages. Such integrated nanosystems are expected to provide a platform for the efficient management of CNS diseases. It is also expected that biomedical research based on nanomaterials will expand into other mental disorders and psychiatric imaging such as schizophrenia, depression, and anxiety disorders, rather than mainly focusing on brain tumors, neurodegenerative diseases, stroke, and epilepsy. Moreover, innovative functionalized nanomaterials are also demanded to be developed for delivering diverse cargos and therapeutic agents such as antibiotics. This could in turn optimize the delivery, application, dosing, targeting, and consequently, future resistance of the drug.

## AUTHOR INFORMATION


### Corresponding Authors

**Ka-Leung Wong** − *The Hong Kong Polytechnic University, Department of Applied Biology and Chemical Technology, Hong Kong SAR 999077, China*; Email: klgwong@polyu.edu.hk

**Angelo Homayoun All** − *Hong Kong Baptist University, Department of Chemistry, Hong Kong SAR 999077, China*; orcid.org/0000-0002-7086-2170; Email: angelo@hkbu.edu.hk

### Authors

**Shuai Zha** − *Hubei University of Chinese Medicine, School of Laboratory Medicine, Wuhan 430065, China; Hubei Shizhen Laboratory, Wuhan 430061, China*

**Haitao Liu** − *Hong Kong Baptist University, Department of Chemistry, Hong Kong SAR 999077, China*

**Hengde Li** − *Hong Kong Baptist University, Department of Chemistry, Hong Kong SAR 999077, China*

**Haolan Li** − *Dalian University of Technology, School of Chemical Engineering, Dalian 116024, China*

Complete contact information is available at: https://pubs.acs.org/10.1021/acsnano.3c10674


### Author Contributions

[▽]Shuai Zha and Haitao Liu contributed equally and share the first authorship. Shuai Zha: investigation, visualization, and writing − original draft; Haitao Liu: investigation, visualization, and writing − original draft; Hengde Li: visualization and writing; Haolan Li: writing; Ka-Leung Wong: supervision and



https://doi.org/10.1021/acsnano.3c10674
ACS Nano 2024, 18, 1820−1845

revision; Angelo Homayoun All: visualization, writing, supervision descriptions, revision, and funding acquisition.

### Notes

The authors declare no competing financial interest.

## ACKNOWLEDGMENTS

This work was supported by the Hong Kong Baptist University: Start-Up Tier 1 Fund (#21.4531.162640; A.H.A.), Faculty Seed Fund (#31.4531.179234; A.H.A.), 2020-22 Initiation Grant for Faculty Niche Research Area, and Research Grant Council 2021-24 General Research Fund (GRF) (# 12100121; A.H.A.). The authors would like to thank Zhili Fan for his limited contribution in this manuscript.

## VOCABULARY

| | |
|---|---|
| homeostasis | the process of maintaining a constant internal environment within the body |
| caveolin | a main integral protein for caveolae |
| hypoxia | low levels of oxygen in the body tissues |
| enhanced permeability and retention | a property that the appropriate sizes of nanoparticles tend to accumulate in tumor tissue much more than in normal tissues |
| clathrin | the principal constituent of a polyhedral protein lattice that coats cell membranes |
| amphiphilicity | the property of some molecules to have an affinity to two phases, polar solvent phase and hydrophobic phase |
| upconversion nanoparticles | a unique class of optical nanomaterials doped with lanthanide ions featuring a wealth of electronic transitions within the 4f electron shells |
| protein corona | the presence of a protein layer on the nanoparticle surface. |

## ABBREVIATIONS

| | |
|---|---|
| BBB | blood−brain barrier |
| CNS | central nervous system |
| NP | nanoparticle |
| EC | endothelial cell |
| TJ | tight junction |
| AMT | adsorptive-mediated transcytosis |
| RMT | receptor-mediated transcytosis |
| PLGA | poly(lactic-*co*-glycolic acid) |
| PEI | polyethylenimine |
| MSN | mesoporous silica nanoparticle |

## REFERENCES

(1) Furtado, D.; Björnmalm, M.; Ayton, S.; Bush, A. I.; Kempe, K.; Caruso, F. Overcoming the blood−brain barrier: the role of nanomaterials in treating neurological diseases. *Adv. Mater.* **2018**, *30* (46), 1801362.

(2) Israel, L. L.; Galstyan, A.; Holler, E.; Ljubimova, J. Y. Magnetic iron oxide nanoparticles for imaging, targeting and treatment of primary and metastatic tumors of the brain. *J. Controlled Release* **2020**, *320*, 45−62.

(3) Xie, J.; Shen, Z.; Anraku, Y.; Kataoka, K.; Chen, X. Nanomaterial-based blood-brain-barrier (BBB) crossing strategies. *Biomaterials* **2019**, *224*, 119491.

(4) Wang, W.; He, H.; Marín-Ramos, N. I.; Zeng, S.; Swenson, S. D.; Cho, H.-Y.; Fu, J.; Beringer, P. M.; Neman, J.; Chen, L.; et al. Enhanced brain delivery and therapeutic activity of trastuzumab after blood-brain barrier opening by NEO100 in mouse models of brain-metastatic breast cancer. *Neuro-Oncology* **2021**, *23* (10), 1656−1667.

(5) Zhang, C.; Song, J.; Lou, L.; Qi, X.; Zhao, L.; Fan, B.; Sun, G.; Lv, Z.; Fan, Z.; Jiao, B.; Yang, J. Doxorubicin-loaded nanoparticle coated with endothelial cells-derived exosomes for immunogenic chemotherapy of glioblastoma. *Bioeng. Transl. Med.* **2021**, *6* (3), No. e10203.

(6) Fu, S.; Liang, M.; Wang, Y.; Cui, L.; Gao, C.; Chu, X.; Liu, Q.; Feng, Y.; Gong, W.; Yang, M.; et al. Dual-modified novel biomimetic nanocarriers improve targeting and therapeutic efficacy in glioma. *ACS Appl. Mater. Interfaces* **2019**, *11* (2), 1841−1854.

(7) Poovaiah, N.; Davoudi, Z.; Peng, H.; Schlichtmann, B.; Mallapragada, S.; Narasimhan, B.; Wang, Q. Treatment of neurodegenerative disorders through the blood−brain barrier using nanocarriers. *Nanoscale* **2018**, *10* (36), 16962−16983.

(8) Tsou, Y. H.; Zhang, X. Q.; Zhu, H.; Syed, S.; Xu, X. Drug delivery to the brain across the blood−brain barrier using nanomaterials. *Small* **2017**, *13* (43), 1701921.

(9) Huang, R.; Zhou, X.; Chen, G.; Su, L.; Liu, Z.; Zhou, P.; Weng, J.; Min, Y. Advances of functional nanomaterials for magnetic resonance imaging and biomedical engineering applications. *Wiley Interdiscip. Rev.: Nanomed. Nanobiotechnol.* **2022**, *14*, No. e1800.

(10) Hwang, H. S.; Jeong, J. W.; Kim, Y. A.; Chang, M. Carbon nanomaterials as versatile platforms for biosensing applications. *Micromachines* **2020**, *11* (9), 814.

(11) Pandit, R.; Chen, L.; Götz, J. The blood-brain barrier: Physiology and strategies for drug delivery. *Adv. Drug Delivery Rev.* **2020**, *165*, 1−14.

(12) Banks, W. A. From blood−brain barrier to blood−brain interface: new opportunities for CNS drug delivery. *Nat. Rev. Drug Discovery* **2016**, *15* (4), 275−292.

(13) Kadry, H.; Noorani, B.; Cucullo, L. A blood−brain barrier overview on structure, function, impairment, and biomarkers of integrity. *Fluids Barriers CNS* **2020**, *17* (1), 69.

(14) Jena, L.; McErlean, E.; McCarthy, H. Delivery across the blood-brain barrier: nanomedicine for glioblastoma multiforme. *Drug Delivery Transl. Res.* **2020**, *10* (2), 304−318.

(15) Haileselassie, B.; Joshi, A. U.; Minhas, P. S.; Mukherjee, R.; Andreasson, K. I.; Mochly-Rosen, D. Mitochondrial dysfunction mediated through dynamin-related protein 1 (Drp1) propagates impairment in blood brain barrier in septic encephalopathy. *J. Neuroinflammation* **2020**, *17* (1), 36.

(16) Lee, M. J.; Zhu, J.; An, J. H.; Lee, S. E.; Kim, T. Y.; Oh, E.; Kang, Y. E.; Chung, W.; Heo, J. Y. A transcriptomic analysis of cerebral microvessels reveals the involvement of Notch1 signaling in endothelial mitochondrial-dysfunction-dependent BBB disruption. *Fluids Barriers CNS* **2022**, *19* (1), 64.

(17) Ding, S.; Khan, A. I.; Cai, X.; Song, Y.; Lyu, Z.; Du, D.; Dutta, P.; Lin, Y. Overcoming blood−brain barrier transport: Advances in nanoparticle-based drug delivery strategies. *Mater. Today* **2020**, *37*, 112−125.

(18) Sweeney, M. D.; Zhao, Z.; Montagne, A.; Nelson, A. R.; Zlokovic, B. V. Blood-brain barrier: from physiology to disease and back. *Physiol. Rev.* **2019**, *99* (1), 21−78.



https://doi.org/10.1021/acsnano.3c10674
*ACS Nano* 2024, 18, 1820−1845

(19) Haddad-Tóvolli, R.; Dragano, N. R. V.; Ramalho, A. F. S.; Velloso, L. A. Development and function of the blood-brain barrier in the context of metabolic control. *Front. Neurosci.* **2017**, *11*, 224.
(20) Heithoff, B. P.; George, K. K.; Phares, A. N.; Zuidhoek, I. A.; Munoz-Ballester, C.; Robel, S. Astrocytes are necessary for blood–brain barrier maintenance in the adult mouse brain. *Glia* **2021**, *69* (2), 436–472.
(21) Knox, E. G.; Aburto, M. R.; Clarke, G.; Cryan, J. F.; O'Driscoll, C. M. The blood-brain barrier in aging and neurodegeneration. *Mol. Psychiatry* **2022**, *27* (6), 2659–2673.
(22) Do, P. T.; Wu, C.-C.; Chiang, Y.-H.; Hu, C.-J.; Chen, K.-Y. Mesenchymal stem/stromal cell therapy in blood–brain barrier preservation following ischemia: Molecular mechanisms and prospects. *Int. J. Mol. Sci.* **2021**, *22* (18), 10045.
(23) Boyé, K.; Geraldo, L. H.; Furtado, J.; Pibouin-Fragner, L.; Poulet, M.; Kim, D.; Nelson, B.; Xu, Y.; Jacob, L.; Maissa, N.; et al. Endothelial Unc5B controls blood-brain barrier integrity. *Nat. Commun.* **2022**, *13* (1), 1169.
(24) Liebner, S.; Dijkhuizen, R. M.; Reiss, Y.; Plate, K. H.; Agalliu, D.; Constantin, G. Functional morphology of the blood–brain barrier in health and disease. *Acta Neuropathol.* **2018**, *135*, 311–336.
(25) Hussain, B.; Fang, C.; Huang, X.; Feng, Z.; Yao, Y.; Wang, Y.; Chang, J. Endothelial $\beta$-catenin deficiency causes blood-brain barrier breakdown via enhancing the paracellular and transcellular permeability. *Front. Mol. Neurosci.* **2022**, *15*, 895429.
(26) Reddy, S.; Tatiparti, K.; Sau, S.; Iyer, A. K. Recent advances in nano delivery systems for blood-brain barrier (BBB) penetration and targeting of brain tumors. *Drug Discovery Today* **2021**, *26* (8), 1944–1952.
(27) Zhou, Y.; Peng, Z.; Seven, E. S.; Leblanc, R. M. Crossing the blood-brain barrier with nanoparticles. *J. Controlled Release* **2018**, *270*, 290–303.
(28) Hu, P.; Lu, Y.; Pan, B.-X.; Zhang, W.-H. New insights into the pivotal role of the amygdala in inflammation-related depression and anxiety disorder. *Int. J. Mol. Sci.* **2022**, *23* (19), 11076.
(29) Abla, K. K.; Mehanna, M. M. The Battle of Lipid-based Nanocarriers Against Blood-brain Barrier: A Critical Review. *J. Drug Targeting* **2023**, *31*, 832.
(30) Anwar, M. M.; Özkan, E.; Gürsoy-Özdemir, Y. The role of extracellular matrix alterations in mediating astrocyte damage and pericyte dysfunction in Alzheimer's disease: A comprehensive review. *Eur. J. Neurosci.* **2022**, *56* (9), 5453–5475.
(31) Hayden, M. R. Brain Endothelial Cells Play a Central Role in the Development of Enlarged Perivascular Spaces in the Metabolic Syndrome. *Medicina* **2023**, *59* (6), 1124.
(32) Yang, L.-Y.; Chen, Y.-R.; Lee, J.-E.; Chen, K.-W.; Luh, H.-T.; Chen, Y.-T.; Wang, K.-C.; Hsieh, S.-T. Dental Pulp Stem Cell-Derived Conditioned Medium Alleviates Subarachnoid Hemorrhage-Induced Microcirculation Impairment by Promoting M2 Microglia Polarization and Reducing Astrocyte Swelling. *Transl. Stroke Res.* **2022**, 688.
(33) Candelario-Jalil, E.; Dijkhuizen, R. M.; Magnus, T. Neuroinflammation, stroke, blood-brain barrier dysfunction, and imaging modalities. *Stroke* **2022**, *53* (5), 1473–1486.
(34) Alkahtani, R. Molecular mechanisms underlying some major common risk factors of stroke. *Heliyon* **2022**, *8*, e10218.
(35) Müller, S.; Kufner, A.; Dell'Orco, A.; Rackoll, T.; Mekle, R.; Piper, S. K.; Fiebach, J. B.; Villringer, K.; Flöel, A.; Endres, M.; et al. Evolution of blood-brain barrier permeability in subacute ischemic stroke and associations with serum biomarkers and functional outcome. *Front. Neurol.* **2021**, *12*, 730923.
(36) Bernardo-Castro, S.; Sousa, J. A.; Martins, E.; Donato, H.; Nunes, C.; d'Almeida, O. C.; Castelo-Branco, M.; Abrunhosa, A.; Ferreira, L.; Sargento-Freitas, J. The evolution of blood–brain barrier permeability changes after stroke and its implications on clinical outcome: A systematic review and meta-analysis. *Int. J. Stroke* **2023**, *18*, 783.
(37) Bernardo-Castro, S.; Sousa, J. A.; Brás, A.; Cecília, C.; Rodrigues, B.; Almendra, L.; Machado, C.; Santo, G.; Silva, F.; Ferreira, L.; et al. Pathophysiology of blood–brain barrier permeability throughout the different stages of ischemic stroke and its implication on hemorrhagic transformation and recovery. *Front. Neurol.* **2020**, *11*, 1605.
(38) Song, S.; Huang, H.; Guan, X.; Fiesler, V.; Bhuiyan, M. I. H.; Liu, R.; Jalali, S.; Hasan, M. N.; Tai, A. K.; Chattopadhyay, A.; et al. Activation of endothelial Wnt/$\beta$-catenin signaling by protective astrocytes repairs BBB damage in ischemic stroke. *Prog. Neurobiol.* **2021**, *199*, 101963.
(39) Bernardo-Castro, S.; Albino, I.; Barrera-Sandoval, Á. M.; Tomatis, F.; Sousa, J. A.; Martins, E.; Simões, S.; Lino, M. M.; Ferreira, L.; Sargento-Freitas, J. Therapeutic nanoparticles for the different phases of ischemic stroke. *Life* **2021**, *11* (6), 482.
(40) Quader, S.; Kataoka, K.; Cabral, H. Nanomedicine for brain cancer. *Adv. Drug Delivery Rev.* **2022**, *182*, 114115.
(41) de Gooijer, M. C.; Kemper, E. M.; Buil, L. C. M.; Çitirikkaya, C. H.; Buckle, T.; Beijnen, J. H.; van Tellingen, O. ATP-binding cassette transporters restrict drug delivery and efficacy against brain tumors even when blood-brain barrier integrity is lost. *Cell Rep. Med.* **2021**, *2* (1), 100184.
(42) Rathi, S.; Griffith, J. I.; Zhang, W.; Zhang, W.; Oh, J. H.; Talele, S.; Sarkaria, J. N.; Elmquist, W. F. The influence of the blood–brain barrier in the treatment of brain tumours. *J. Intern. Med.* **2022**, *292* (1), 3–30.
(43) Sarkaria, J. N.; Hu, L. S.; Parney, I. F.; Pafundi, D. H.; Brinkmann, D. H.; Laack, N. N.; Giannini, C.; Burns, T. C.; Kizilbash, S. H.; Laramy, J. K.; et al. Is the blood–brain barrier really disrupted in all glioblastomas? A critical assessment of existing clinical data. *Neuro-Oncology* **2018**, *20* (2), 184–191.
(44) Cai, Q.; Li, X.; Xiong, H.; Fan, H.; Gao, X.; Vemireddy, V.; Margolis, R.; Li, J.; Ge, X.; Giannotta, M.; et al. Optical blood-brain-tumor barrier modulation expands therapeutic options for glioblastoma treatment. *Nat. Commun.* **2023**, *14* (1), 4934.
(45) Morris, E. K.; Daignault-Mill, S.; Stehbens, S. J.; Genovesi, L. A.; Lagendijk, A. K. Addressing blood-brain-tumor-barrier heterogeneity in pediatric brain tumors with innovative preclinical models. *Front. Oncol.* **2023**, *13*, 1101522.
(46) Wu, W.; Klockow, J. L.; Zhang, M.; Lafortune, F.; Chang, E.; Jin, L.; Wu, Y.; Daldrup-Link, H. E. Glioblastoma multiforme (GBM): An overview of current therapies and mechanisms of resistance. *Pharmacol. Res.* **2021**, *171*, 105780.
(47) Wolburg, H.; Wolburg-Buchholz, K.; Kraus, J.; Rascher-Eggstein, G.; Liebner, S.; Hamm, S.; Duffner, F.; Grote, E.-H.; Risau, W.; Engelhardt, B. Localization of claudin-3 in tight junctions of the blood-brain barrier is selectively lost during experimental autoimmune encephalomyelitis and human glioblastoma multiforme. *Acta Neuropathol.* **2003**, *105*, 586–592.
(48) Song, Y.; Hu, C.; Fu, Y.; Gao, H. Modulating the blood–brain tumor barrier for improving drug delivery efficiency and efficacy. *View* **2022**, *3* (1), 20200129.
(49) Khan, I.; Baig, M. H.; Mahfooz, S.; Imran, M. A.; Khan, M. I.; Dong, J.-J.; Cho, J. Y.; Hatiboglu, M. A. Nanomedicine for glioblastoma: progress and future prospects. *Semin. Cancer Biol.*; Elsevier, 2022.
(50) Macedo-Pereira, A.; Martins, C.; Lima, J.; Sarmento, B. Digging the intercellular crosstalk via extracellular vesicles: May exosomes be the drug delivery solution for target glioblastoma? *J. Controlled Release* **2023**, *358*, 98–115.
(51) Hersh, A. M.; Alomari, S.; Tyler, B. M. Crossing the blood-brain barrier: advances in nanoparticle technology for drug delivery in neuro-oncology. *Int. J. Mol. Sci.* **2022**, *23* (8), 4153.
(52) Li, J.; Wang, X.; Guo, Y.; Zhang, Y.; Zhu, A.; Zeng, W.; Di, L.; Wang, R. Ginsenoside Rg3-engineered exosomes as effective delivery platform for potentiated chemotherapy and photoimmunotherapy of glioblastoma. *Chem. Eng. J.* **2023**, *471*, 144692.
(53) Liu, W.-S.; Wu, L.-L.; Chen, C.-M.; Zheng, H.; Gao, J.; Lu, Z.-M.; Li, M. Lipid-hybrid cell-derived biomimetic functional materials: A state-of-the-art multifunctional weapon against tumors. *Materials Today Bio* **2023**, *22*, 100751.


https://doi.org/10.1021/acsnano.3c10674
*ACS Nano* 2024, 18, 1820–1845

(54) Chin, K. S. Pathophysiology of dementia. *Aust. J. Gen. Pract.* **2023**, *52* (8), 516.
(55) Khan, F.; Qiu, H. Amyloid-$\beta$: A potential mediator of aging-related vascular pathologies. *Vasc. Pharmacol.* **2023**, *152*, 107213.
(56) Li, P.; Fan, H. Pericyte Loss in Diseases. *Cells* **2023**, *12* (15), 1931.
(57) Farfara, D.; Sooliman, M.; Avrahami, L.; Royal, T. G.; Amram, S.; Rozenstein-Tsalkovich, L.; Trudler, D.; Blanga-Kanfi, S.; Eldar-Finkelman, H.; Pahnke, J.; et al. Physiological expression of mutated TAU impaired astrocyte activity and exacerbates $\beta$-amyloid pathology in 5xFAD mice. *J. Neuroinflammation* **2023**, *20* (1), 174.
(58) Huang, X. *Alzheimer's Disease: Drug Discovery*; Exon Publications: Brisbane, Australia, 2020.
(59) Bennett, R. E.; Robbins, A. B.; Hu, M.; Cao, X.; Betensky, R. A.; Clark, T.; Das, S.; Hyman, B. T. Tau induces blood vessel abnormalities and angiogenesis-related gene expression in P301L transgenic mice and human Alzheimer's disease. *Proc. Natl. Acad. Sci. U. S. A.* **2018**, *115* (6), E1289.
(60) Michalicova, A.; Majerova, P.; Kovac, A. Tau protein and its role in blood–brain barrier dysfunction. *Front. Mol. Neurosci.* **2020**, *13*, 570045.
(61) Yue, Q.; Hoi, M. P. M. Emerging roles of astrocytes in blood-brain barrier disruption upon amyloid-beta insults in Alzheimer's disease. *Neural Regener. Res.* **2023**, *18* (9), 1890.
(62) Sweeney, M. D.; Sagare, A. P.; Zlokovic, B. V. Blood–brain barrier breakdown in Alzheimer disease and other neurodegenerative disorders. *Nat. Rev. Neurol.* **2018**, *14* (3), 133–150.
(63) Vázquez-Vélez, G. E.; Zoghbi, H. Y. Parkinson's disease genetics and pathophysiology. *Annu. Rev. Neurosci.* **2021**, *44*, 87–108.
(64) Matsuoka, R. L.; Buck, L. D.; Vajrala, K. P.; Quick, R. E.; Card, O. A. Historical and current perspectives on blood endothelial cell heterogeneity in the brain. *Cell. Mol. Life Sci.* **2022**, *79* (7), 372.
(65) Gray, M. T.; Woulfe, J. M. Striatal blood–brain barrier permeability in Parkinson's disease. *J. Cereb. Blood Flow Metab.* **2015**, *35* (5), 747–750.
(66) de Rus Jacquet, A.; Alpaugh, M.; Denis, H. L.; Tancredi, J. L.; Boutin, M.; Decaestecker, J.; Beauparlant, C.; Herrmann, L.; Saint-Pierre, M.; Parent, M.; et al. The contribution of inflammatory astrocytes to BBB impairments in a brain-chip model of Parkinson's disease. *Nat. Commun.* **2023**, *14* (1), 3651.
(67) Argaw, A. T.; Asp, L.; Zhang, J.; Navrazhina, K.; Pham, T.; Mariani, J. N.; Mahase, S.; Dutta, D. J.; Seto, J.; Kramer, E. G.; et al. Astrocyte-derived VEGF-A drives blood-brain barrier disruption in CNS inflammatory disease. *J. Clin. Invest.* **2012**, *122* (7), 2454–2468.
(68) Pienaar, I. S.; Lee, C. H.; Elson, J. L.; McGuinness, L.; Gentleman, S. M.; Kalaria, R. N.; Dexter, D. T. Deep-brain stimulation associates with improved microvascular integrity in the subthalamic nucleus in Parkinson's disease. *Neurobiol. Dis.* **2015**, *74*, 392–405.
(69) Bartels, A. L.; Willemsen, A. T. M.; Kortekaas, R.; De Jong, B. M.; De Vries, R.; De Klerk, O.; Van Oostrom, J. C. H.; Portman, A.; Leenders, K. L. Decreased blood–brain barrier P-glycoprotein function in the progression of Parkinson's disease, PSP and MSA. *J. Neural Transm.* **2008**, *115*, 1001–1009.
(70) Al-Bachari, S.; Naish, J. H.; Parker, G. J. M.; Emsley, H. C. A.; Parkes, L. M. Blood–brain barrier leakage is increased in Parkinson's disease. *Front. Physiol.* **2020**, *11*, 593026.
(71) Herda, L. M.; Polo, E.; Kelly, P. M.; Rocks, L.; Hudecz, D.; Dawson, K. A. Designing the future of nanomedicine: current barriers to targeted brain therapeutics. *Eur. J. Nanomed.* **2014**, *6* (3), 127–139.
(72) Lalatsa, A.; Butt, A. M., Physiology of the blood–brain barrier and mechanisms of transport across the BBB. In *Nanotechnology-Based Targeted Drug Delivery Systems for Brain Tumors*; Elsevier: 2018; pp 49–74.
(73) Chen, S.; Zhou, Q.; Wang, G.; Zhou, Z.; Tang, J.; Xie, T.; Shen, Y. Effect of Cationic Charge Density on Transcytosis of Polyethylenimine. *Biomacromolecules* **2021**, *22* (12), 5139–5150.
(74) Song, J.; Lu, C.; Leszek, J.; Zhang, J. Design and Development of Nanomaterial-Based Drug Carriers to Overcome the Blood–Brain Barrier by Using Different Transport Mechanisms. *Int. J. Mol. Sci.* **2021**, *22* (18), 10118.
(75) Zhao, F.; Zhong, L.; Luo, Y. Endothelial glycocalyx as an important factor in composition of blood-brain barrier. *CNS Neurosci. Ther.* **2021**, *27* (1), 26–35.
(76) Zhang, W.; Liu, Q. Y.; Haqqani, A. S.; Leclerc, S.; Liu, Z.; Fauteux, F.; Baumann, E.; Delaney, C. E.; Ly, D.; Star, A. T.; et al. Differential expression of receptors mediating receptor-mediated transcytosis (RMT) in brain microvessels, brain parenchyma and peripheral tissues of the mouse and the human. *Fluids Barriers CNS* **2020**, *17* (1), 47.
(77) Villaseñor, R.; Lampe, J.; Schwaninger, M.; Collin, L. Intracellular transport and regulation of transcytosis across the blood–brain barrier. *Cell. Mol. Life Sci.* **2019**, *76* (6), 1081–1092.
(78) Kaksonen, M.; Roux, A. Mechanisms of clathrin-mediated endocytosis. *Nat. Rev. Mol. Cell Biol.* **2018**, *19* (5), 313–326.
(79) Yang, C.; He, B.; Dai, W.; Zhang, H.; Zheng, Y.; Wang, X.; Zhang, Q. The role of caveolin-1 in the biofate and efficacy of anti-tumor drugs and their nano-drug delivery systems. *Acta Pharm. Sin. B* **2021**, *11* (4), 961–977.
(80) Parton, R. G. Caveolae: structure, function, and relationship to disease. *Annu. Rev. Cell Dev. Biol.* **2018**, *34*, 111–136.
(81) Balzer, V.; Poc, P.; Puris, E.; Martin, S.; Aliasgari, M.; Auriola, S.; Fricker, G. Re-evaluation of the hCMEC/D3 based in vitro BBB model for ABC transporter studies. *Eur. J. Pharm. Biopharm.* **2022**, *173*, 12–21.
(82) Zhang, W.; Sigdel, G.; Mintz, K. J.; Seven, E. S.; Zhou, Y.; Wang, C.; Leblanc, R. M. Carbon dots: A future Blood–Brain Barrier penetrating nanomedicine and drug nanocarrier. *Int. J. Nanomed.* **2021**, *16*, 5003–5016.
(83) Lombardo, S. M.; Schneider, M.; Türeli, A. E.; Günday Türeli, N. G. Key for crossing the BBB with nanoparticles: The rational design. *Beilstein J. Nanotechnol.* **2020**, *11* (1), 866–883.
(84) Lakshmipriya, T.; Gopinath, S. C. B. Introduction to nanoparticles and analytical devices. In *Nanopart. Anal. Med. Devices*; Elsevier: 2021; pp 1–29.
(85) Sokolova, V.; Mekky, G.; van der Meer, S. B.; Seeds, M. C.; Atala, A. J.; Epple, M. Transport of ultrasmall gold nanoparticles (2 nm) across the blood–brain barrier in a six-cell brain spheroid model. *Sci. Rep.* **2020**, *10* (1), 18033.
(86) Sela, H.; Cohen, H.; Elia, P.; Zach, R.; Karpas, Z.; Zeiri, Y. Spontaneous penetration of gold nanoparticles through the blood brain barrier (BBB). *J. Nanobiotechnol.* **2015**, *13* (1), 71.
(87) Guo, F.; Li, Q.; Zhang, X.; Liu, Y.; Jiang, J.; Cheng, S.; Yu, S.; Zhang, X.; Liu, F.; Li, Y.; et al. Applications of Carbon Dots for the Treatment of Alzheimer's Disease. *Int. J. Nanomed.* **2022**, *17*, 6621–6638.
(88) Zhou, Y.; Kandel, N.; Bartoli, M.; Serafim, L. F.; ElMetwally, A. E.; Falkenberg, S. M.; Paredes, X. E.; Nelson, C. J.; Smith, N.; Padovano, E.; et al. Structure-activity relationship of carbon nitride dots in inhibiting Tau aggregation. *Carbon* **2022**, *193*, 1–16.
(89) Zhou, Y.; Liyanage, P. Y.; Devadoss, D.; Rios Guevara, L. R. R.; Cheng, L.; Graham, R. M.; Chand, H. S.; Al-Youbi, A. O.; Bashammakh, A. S.; El-Shahawi, M. S.; Leblanc, R. M. Nontoxic amphiphilic carbon dots as promising drug nanocarriers across the blood–brain barrier and inhibitors of $\beta$-amyloid. *Nanoscale* **2019**, *11* (46), 22387–22397.
(90) Deng, K.; Zhang, L.; Gao, W.; Lin, X.; Long, X.; Wang, Y.; Wu, M. A Functional Carbon Dots Induce Ferroptosis By Suppressing PLPP4 Activity to Inhibit Glioblastoma Growth. *Chem. Eng. J.***2023**, *475146473*
(91) Amiri, M.; Jafari, S.; Kurd, M.; Mohamadpour, H.; Khayati, M.; Ghobadinezhad, F.; Tavallaei, O.; Derakhshankhah, H.; Sadegh Malvajerd, S.; Izadi, Z. Engineered solid lipid nanoparticles and nanostructured lipid carriers as new generations of blood–brain barrier transmitters. *ACS Chem. Neurosci.* **2021**, *12* (24), 4475–4490.
(92) Jnaidi, R.; Almeida, A. J.; Gonçalves, L. M. Solid lipid nanoparticles and nanostructured lipid carriers as smart drug delivery


https://doi.org/10.1021/acsnano.3c10674
*ACS Nano* 2024, 18, 1820–1845

systems in the treatment of glioblastoma multiforme. *Pharmaceutics* **2020**, *12* (9), 860.
(93) Ghouri, M. D.; Saleem, J.; Ren, J.; Liu, J.; Umer, A.; Cai, R.; Chen, C. Nanomaterials-Mediated Structural and Physiological Modulation of Blood Brain Barrier for Therapeutic Purposes. *Adv. Mater. Interfaces* **2022**, *9* (1), 2101391.
(94) Sommonte, F.; Arduino, I.; Racaniello, G. F.; Lopalco, A.; Lopedota, A. A.; Denora, N. The Complexity of the Blood-Brain Barrier and the Concept of Age-Related Brain Targeting: Challenges and Potential of Novel Solid Lipid-Based Formulations. *J. Pharm. Sci.* **2022**, *111* (3), 577−592.
(95) Garg, J.; Pathania, K.; Sah, S. P.; Pawar, S. V. Nanostructured lipid carriers: a promising drug carrier for targeting brain tumours. *Futur. J. Pharm. Sci.* **2022**, *8* (1), 25.
(96) Akanda, M.; Mithu, M. D. S. H.; Douroumis, D. Solid lipid nanoparticles: An effective lipid-based technology for cancer treatment. *J. Drug Delivery Sci. Technol.* **2023**, *86*, 104709.
(97) Jagaran, K.; Singh, M. Lipid nanoparticles: promising treatment approach for Parkinson's disease. *International Int. J. Mol. Sci.* **2022**, *23* (16), 9361.
(98) Shivananjegowda, M. G.; Hani, U.; Osmani, R. A. M.; Alamri, A. H.; Ghazwani, M.; Alhamhoom, Y.; Rahamathulla, M.; Paranthaman, S.; Gowda, D. V.; Siddiqua, A. Development and Evaluation of Solid Lipid Nanoparticles for the Clearance of A$\beta$ in Alzheimer's Disease. *Pharmaceutics* **2023**, *15* (1), 221.
(99) Akel, H.; Ismail, R.; Katona, G.; Sabir, F.; Ambrus, R.; Csóka, I. A comparison study of lipid and polymeric nanoparticles in the nasal delivery of meloxicam: Formulation, characterization, and in vitro evaluation. *Int. J. Pharm.* **2021**, *604*, 120724.
(100) Costa, C. P.; Moreira, J. N.; Sousa Lobo, J. M. S.; Silva, A. C. Intranasal delivery of nanostructured lipid carriers, solid lipid nanoparticles and nanoemulsions: A current overview of in vivo studies. *Acta Pharm. Sin. B* **2021**, *11* (4), 925−940.
(101) Akel, H.; Csóka, I.; Ambrus, R.; Bocsik, A.; Gróf, I.; Mészáros, M.; Szecskó, A.; Kozma, G.; Veszelka, S.; Deli, M. A.; et al. In vitro comparative study of solid lipid and PLGA nanoparticles designed to facilitate nose-to-Brain delivery of insulin. *Int. J. Mol. Sci.* **2021**, *22* (24), 13258.
(102) Akel, H.; Csóka, I. Formulation and In Vitro Comparison Study between Lipid-Based and Polymeric-Based Nanoparticles for Nose-to-Brain Delivery of a Model Drug for Alzheimer's Disease. *Proceedings* **2020**, 51.
(103) Zhou, Y.; Zhu, F.; Liu, Y.; Zheng, M.; Wang, Y.; Zhang, D.; Anraku, Y.; Zou, Y.; Li, J.; Wu, H.; et al. Blood-brain barrier−penetrating siRNA nanomedicine for Alzheimer's disease therapy. *Sci. Adv.* **2020**, *6* (41), No. eabc7031.
(104) Arora, S.; Sharma, D.; Singh, J. GLUT-1: an effective target to deliver brain-derived neurotrophic factor gene across the blood brain barrier. *ACS Chem. Neurosci.* **2020**, *11* (11), 1620−1633.
(105) Gonzalez-Carter, D. A.; Ong, Z. Y.; McGilvery, C. M.; Dunlop, I. E.; Dexter, D. T.; Porter, A. E. L-DOPA functionalized, multi-branched gold nanoparticles as brain-targeted nano-vehicles. *Nanomedicine* **2019**, *15* (1), 1−11.
(106) Fernandes, J.; Ghate, M. V.; Basu Mallik, S.; Lewis, S. A. Amino acid conjugated chitosan nanoparticles for the brain targeting of a model dipeptidyl peptidase-4 inhibitor. *Int. J. Pharm.* **2018**, *547* (1−2), 563−571.
(107) Muniswamy, V. J.; Raval, N.; Gondaliya, P.; Tambe, V.; Kalia, K.; Tekade, R. K. 'Dendrimer-Cationized-Albumin'encrusted polymeric nanoparticle improves BBB penetration and anticancer activity of doxorubicin. *Int. J. Pharm.* **2019**, *555*, 77−99.
(108) Piazzini, V.; Landucci, E.; Graverini, G.; Pellegrini-Giampietro, D. E.; Bilia, A. R.; Bergonzi, M. C. Stealth and cationic nanoliposomes as drug delivery systems to increase andrographolide BBB permeability. *Pharmaceutics* **2018**, *10* (3), 128.
(109) Piazzini, V.; Landucci, E.; D'Ambrosio, M.; Tiozzo Fasiolo, L.; Cinci, L.; Colombo, G.; Pellegrini-Giampietro, D. E.; Bilia, A. R.; Luceri, C.; Bergonzi, M. C. Chitosan coated human serum albumin nanoparticles: A promising strategy for nose-to-brain drug delivery. *Int. J. Biol. Macromol.* **2019**, *129*, 267−280.
(110) Fan, K.; Jia, X.; Zhou, M.; Wang, K.; Conde, J.; He, J.; Tian, J.; Yan, X. Ferritin nanocarrier traverses the blood brain barrier and kills glioma. *ACS Nano* **2018**, *12* (5), 4105−4115.
(111) Janjua, T. I.; Ahmed-Cox, A.; Meka, A. K.; Mansfeld, F. M.; Forgham, H.; Ignacio, R. M. C.; Cao, Y.; McCarroll, J. A.; Mazzieri, R.; Kavallaris, M.; Popat, A. Facile synthesis of lactoferrin conjugated ultra small large pore silica nanoparticles for the treatment of glioblastoma. *Nanoscale* **2021**, *13* (40), 16909−16922.
(112) Zhong, G.; Long, H.; Zhou, T.; Liu, Y.; Zhao, J.; Han, J.; Yang, X.; Yu, Y.; Chen, F.; Shi, S. Blood-brain barrier Permeable nanoparticles for Alzheimer's disease treatment by selective mitophagy of microglia. *Biomaterials* **2022**, *288*, 121690.
(113) Guo, Q.; Zhu, Q.; Miao, T.; Tao, J.; Ju, X.; Sun, Z.; Li, H.; Xu, G.; Chen, H.; Han, L. LRP1-upregulated nanoparticles for efficiently conquering the blood-brain barrier and targetedly suppressing multifocal and infiltrative brain metastases. *J. Controlled Release* **2019**, *303*, 117−129.
(114) Ahn, S. I.; Sei, Y. J.; Park, H.-J.; Kim, J.; Ryu, Y.; Choi, J. J.; Sung, H.-J.; MacDonald, T. J.; Levey, A. I.; Kim, Y. Microengineered human blood−brain barrier platform for understanding nanoparticle transport mechanisms. *Nat. Commun.* **2020**, *11* (1), 175.
(115) Niu, W.; Xiao, Q.; Wang, X.; Zhu, J.; Li, J.; Liang, X.; Peng, Y.; Wu, C.; Lu, R.; Pan, Y.; et al. A biomimetic drug delivery system by integrating grapefruit extracellular vesicles and doxorubicin-loaded heparin-based nanoparticles for glioma therapy. *Nano Lett.* **2021**, *21* (3), 1484−1492.
(116) Gomes, M. J.; Kennedy, P. J.; Martins, S.; Sarmento, B. Delivery of siRNA silencing P-gp in peptide-functionalized nanoparticles causes efflux modulation at the blood−brain barrier. *Nanomedicine* **2017**, *12* (12), 1385−1399.
(117) Fernandes, C.; Martins, C.; Fonseca, A.; Nunes, R.; Matos, M. J. o.; Silva, R.; Garrido, J.; Sarmento, B.; Remião, F.; Otero-Espinar, F. J.; et al. PEGylated PLGA nanoparticles as a smart carrier to increase the cellular uptake of a coumarin-based monoamine oxidase B inhibitor. *ACS Appl. Mater. Interfaces* **2018**, *10* (46), 39557−39569.
(118) Stocchetti, N.; Maas, A. I. R. Traumatic intracranial hypertension. *N. Engl. J. Med.* **2014**, *370* (22), 2121−2130.
(119) Lesniak, W. G.; Chu, C.; Jablonska, A.; Behnam Azad, B.; Zwaenepoel, O.; Zawadzki, M.; Lisok, A.; Pomper, M. G.; Walczak, P.; Gettemans, J.; Janowski, M. PET imaging of distinct brain uptake of a nanobody and similarly-sized PAMAM dendrimers after intra-arterial administration. *Eur. J. Nucl. Med. Mol. Imaging* **2019**, *46* (9), 1940−1951.
(120) Chu, C.; Jablonska, A.; Lesniak, W. G.; Thomas, A. M.; Lan, X.; Linville, R. M.; Li, S.; Searson, P. C.; Liu, G.; Pearl, M.; et al. Optimization of osmotic blood-brain barrier opening to enable intravital microscopy studies on drug delivery in mouse cortex. *J. Controlled Release* **2020**, *317*, 312−321.
(121) Lesniak, W. G.; Chu, C.; Jablonska, A.; Du, Y.; Pomper, M. G.; Walczak, P.; Janowski, M. A distinct advantage to intraarterial delivery of 89Zr-bevacizumab in PET imaging of mice with and without osmotic opening of the blood−brain barrier. *J. Nucl. Med.* **2019**, *60* (5), 617−622.
(122) Gorick, C. M.; Sheybani, N. D.; Curley, C. T.; Price, R. J. Listening in on the microbubble crowd: advanced acoustic monitoring for improved control of blood-brain barrier opening with focused ultrasound. *Theranostics* **2018**, *8* (11), 2988−2991.
(123) Deng, Z.; Wang, J.; Xiao, Y.; Li, F.; Niu, L.; Liu, X.; Meng, L.; Zheng, H. Ultrasound-mediated augmented exosome release from astrocytes alleviates amyloid-$\beta$-induced neurotoxicity. *Theranostics* **2021**, *11* (9), 4351−4362.
(124) Qu, F.; Wang, P.; Zhang, K.; Shi, Y.; Li, Y.; Li, C.; Lu, J.; Liu, Q.; Wang, X. Manipulation of Mitophagy by "All-in-One" nanosensitizer augments sonodynamic glioma therapy. *Autophagy* **2020**, *16* (8), 1413−1435.


https://doi.org/10.1021/acsnano.3c10674
*ACS Nano* 2024, 18, 1820−1845

(125) Timbie, K. F.; Mead, B. P.; Price, R. J. Drug and gene delivery across the blood−brain barrier with focused ultrasound. *J. Controlled Release* **2015**, *219*, 61−75.
(126) Gorick, C. M.; Sheybani, N. D.; Curley, C. T.; Price, R. J. Listening in on the microbubble crowd: advanced acoustic monitoring for improved control of blood-brain barrier opening with focused ultrasound. *Theranostics* **2018**, *8* (11), 2988.
(127) Mead, B. P.; Curley, C. T.; Kim, N.; Negron, K.; Garrison, W. J.; Song, J.; Rao, D.; Miller, G. W.; Mandell, J. W.; Purow, B. W.; et al. Focused ultrasound preconditioning for augmented nanoparticle penetration and efficacy in the central nervous system. *Small* **2019**, *15* (49), 1903460.
(128) Gasca-Salas, C.; Fernández-Rodríguez, B.; Pineda-Pardo, J. A.; Rodríguez-Rojas, R.; Obeso, I.; Hernández-Fernández, F.; Del Álamo, M.; Mata, D.; Guida, P.; Ordás-Bandera, C.; et al. Blood-brain barrier opening with focused ultrasound in Parkinson's disease dementia. *Nat. Commun.* **2021**, *12* (1), 779.
(129) Pineda-Pardo, J. A.; Gasca-Salas, C.; Fernández-Rodríguez, B.; Rodríguez-Rojas, R.; Del Alamo, M.; Obeso, I.; Hernández-Fernández, F.; Trompeta, C.; Martínez-Fernández, R.; Matarazzo, M.; et al. Striatal Blood−Brain Barrier Opening in Parkinson's Disease Dementia: A Pilot Exploratory Study. *Mov. Disord.* **2022**, *37* (10), 2057−2065.
(130) Li, X.; Vemireddy, V.; Cai, Q.; Xiong, H.; Kang, P.; Li, X.; Giannotta, M.; Hayenga, H. N.; Pan, E.; Sirsi, S. R.; et al. Reversibly modulating the blood−brain barrier by laser stimulation of molecular-targeted nanoparticles. *Nano Lett.* **2021**, *21* (22), 9805−9815.
(131) Hallam, K. A.; Emelianov, S. Y. Toward optimization of blood brain barrier opening induced by laser-activated perfluorocarbon nanodroplets. *Biomed. Opt. Express* **2019**, *10* (7), 3139−3151.
(132) Qiao, R.; Fu, C.; Forgham, H.; Javed, I.; Huang, X.; Zhu, J.; Whittaker, A. K.; Davis, T. P. Magnetic Iron Oxide Nanoparticles for Brain Imaging and Drug Delivery. *Adv. Drug Delivery Rev.* **2023**, *197*, 114822.
(133) Thomsen, L. B.; Linemann, T.; Pondman, K. M.; Lichota, J.; Kim, K. S.; Pieters, R. J.; Visser, G. M.; Moos, T. Uptake and transport of superparamagnetic iron oxide nanoparticles through human brain capillary endothelial cells. *ACS Chem. Neurosci.* **2013**, *4* (10), 1352−1360.
(134) Chertok, B.; Moffat, B. A.; David, A. E.; Yu, F.; Bergemann, C.; Ross, B. D.; Yang, V. C. Iron oxide nanoparticles as a drug delivery vehicle for MRI monitored magnetic targeting of brain tumors. *Biomaterials* **2008**, *29* (4), 487−496.
(135) Qiu, Y.; Tong, S.; Zhang, L.; Sakurai, Y.; Myers, D. R.; Hong, L.; Lam, W. A.; Bao, G. Magnetic forces enable controlled drug delivery by disrupting endothelial cell-cell junctions. *Nat. Commun.* **2017**, *8* (1), 15594.
(136) D'Agata, F.; Ruffinatti, F. A.; Boschi, S.; Stura, I.; Rainero, I.; Abollino, O.; Cavalli, R.; Guiot, C. Magnetic nanoparticles in the central nervous system: targeting principles, applications and safety issues. *Molecules* **2018**, *23* (1), 9.
(137) Chen, J.; Yuan, M.; Madison, C. A.; Eitan, S.; Wang, Y. Blood-brain barrier crossing using magnetic stimulated nanoparticles. *J. Controlled Release* **2022**, *345*, 557−571.
(138) Gupta, R.; Chauhan, A.; Kaur, T.; Kuanr, B. K.; Sharma, D. Transmigration of magnetite nanoparticles across the blood−brain barrier in a rodent model: influence of external and alternating magnetic fields. *Nanoscale* **2022**, *14* (47), 17589−17606.
(139) Gkountas, A. A.; Polychronopoulos, N. D.; Sofiadis, G. N.; Karvelas, E. G.; Spyrou, L. A.; Sarris, I. E. Simulation of magnetic nanoparticles crossing through a simplified blood-brain barrier model for Glioblastoma multiforme treatment. *Comput. Methods Programs Biomed.* **2021**, *212*, 106477.
(140) Tabatabaei, S. N.; Girouard, H.; Carret, A.-S.; Martel, S. Remote control of the permeability of the blood−brain barrier by magnetic heating of nanoparticles: a proof of concept for brain drug delivery. *J. Controlled Release* **2015**, *206*, 49−57.
(141) Chen, Y.; Liu, L. Modern methods for delivery of drugs across the blood−brain barrier. *Adv. Drug Delivery Rev.* **2012**, *64* (7), 640−665.
(142) Terstappen, G. C.; Meyer, A. H.; Bell, R. D.; Zhang, W. Strategies for delivering therapeutics across the blood−brain barrier. *Nat. Rev. Drug Discovery* **2021**, *20* (5), 362−383.
(143) Li, Y.; Teng, X.; Wang, Y.; Yang, C.; Yan, X.; Li, J. Neutrophil delivered hollow titania covered persistent luminescent nanosensitizer for ultrosound augmented chemo/immuno glioblastoma therapy. *Adv. Sci.* **2021**, *8* (17), 2004381.
(144) Deng, Z.; Wang, J.; Xiao, Y.; Li, F.; Niu, L.; Liu, X.; Meng, L.; Zheng, H. Ultrasound-mediated augmented exosome release from astrocytes alleviates amyloid-$\beta$-induced neurotoxicity. *Theranostics* **2021**, *11* (9), 4351.
(145) Chu, C.; Jablonska, A.; Gao, Y.; Lan, X.; Lesniak, W. G.; Liang, Y.; Liu, G.; Li, S.; Magnus, T.; Pearl, M.; et al. Hyperosmolar blood−brain barrier opening using intra-arterial injection of hyperosmotic mannitol in mice under real-time MRI guidance. *Nat. Protoc.* **2022**, *17* (1), 76−94.
(146) Vore, A. S.; Barney, T. M.; Deak, M. M.; Varlinskaya, E. I.; Deak, T. Adolescent intermittent ethanol exposure produces Sex-Specific changes in BBB Permeability: A potential role for VEGFA. *Brain, Behav., Immun.* **2022**, *102*, 209−223.
(147) Zhou, M.-Y.; Zhang, Y.-J.; Ding, H.-M.; Wu, W.-F.; Cai, W.-W.; Wang, Y.-Q.; Geng, D.-Q. Diprotin A TFA Exerts Neurovascular Protection in Ischemic Cerebral Stroke. *Front. Neurosci.* **2022**, *16*, 861059.
(148) Ogawa, K.; Kato, N.; Yoshida, M.; Hiu, T.; Matsuo, T.; Mizukami, S.; Omata, D.; Suzuki, R.; Maruyama, K.; Mukai, H.; Kawakami, S. Focused ultrasound/microbubbles-assisted BBB opening enhances LNP-mediated mRNA delivery to brain. *J. Controlled Release* **2022**, *348*, 34−41.
(149) Meng, Q.; Meng, H.; Pan, Y.; Liu, J.; Li, J.; Qi, Y.; Huang, Y. Influence of nanoparticle size on blood−brain barrier penetration and the accumulation of anti-seizure medicines in the brain. *J. Mater. Chem. B* **2022**, *10* (2), 271−281.
(150) Wang, J.; Zha, M.; Zhao, H.; Yue, W.; Wu, D.; Li, K. Detection of Kidney Dysfunction through In Vivo Magnetic Resonance Imaging with Renal-Clearable Gadolinium Nanoprobes. *Anal. Chem.* **2022**, *94* (9), 4005−4011.
(151) Ozcicek, I.; Aysit, N.; Cakici, C.; Aydeger, A. The effects of surface functionality and size of gold nanoparticles on neuronal toxicity, apoptosis, ROS production and cellular/suborgan biodistribution. *Mater. Sci. Eng. C.* **2021**, *128*, 112308.
(152) Xia, Q.; Huang, J.; Feng, Q.; Chen, X.; Liu, X.; Li, X.; Zhang, T.; Xiao, S.; Li, H.; Zhong, Z.; Xiao, K. Size-and cell type-dependent cellular uptake, cytotoxicity and in vivo distribution of gold nanoparticles. *Int. J. Nanomed.* **2019**, *14*, 6957−6970.
(153) Meena, J.; Gupta, A.; Ahuja, R.; Singh, M.; Bhaskar, S.; Panda, A. K. Inorganic nanoparticles for natural product delivery: A review. *Environ. Chem. Lett.* **2020**, *18*, 2107−2118.
(154) Zhang, W.; Mehta, A.; Tong, Z.; Esser, L.; Voelcker, N. H. Development of polymeric nanoparticles for blood−brain barrier transfer—strategies and challenges. *Adv. Sci.* **2021**, *8* (10), 2003937.
(155) Sonavane, G.; Tomoda, K.; Makino, K. Biodistribution of colloidal gold nanoparticles after intravenous administration: effect of particle size. *Colloids Surf., B* **2008**, *66* (2), 274−280.
(156) Lin, Z.; Xi, L.; Chen, S.; Tao, J.; Wang, Y.; Chen, X.; Li, P.; Wang, Z.; Zheng, Y. Uptake and trafficking of different sized PLGA nanoparticles by dendritic cells in imiquimod-induced psoriasis-like mice model. *Acta Pharm. Sin. B* **2021**, *11* (4), 1047−1055.
(157) Darquenne, C. Deposition mechanisms. *J. Aerosol Med. Pulm. Drug Delivery* **2020**, *33* (4), 181−185.
(158) Betzer, O.; Shilo, M.; Opochinsky, R.; Barnoy, E.; Motiei, M.; Okun, E.; Yadid, G.; Popovtzer, R. The effect of nanoparticle size on the ability to cross the blood−brain barrier: an in vivo study. *Nanomedicine* **2017**, *12* (13), 1533−1546.
(159) Cai, X.; Bandla, A.; Mao, D.; Feng, G.; Qin, W.; Liao, L. D.; Thakor, N.; Tang, B. Z.; Liu, B. Biocompatible Red Fluorescent


https://doi.org/10.1021/acsnano.3c10674
*ACS Nano* 2024, 18, 1820−1845

Organic Nanoparticles with Tunable Size and Aggregation-Induced Emission for Evaluation of Blood−Brain Barrier Damage. *Adv. Mater.* **2016**, *28* (39), 8760−8765.
(160) Nowak, M.; Brown, T. D.; Graham, A.; Helgeson, M. E.; Mitragotri, S. Size, shape, and flexibility influence nanoparticle transport across brain endothelium under flow. *Bioeng. Transl. Med.* **2020**, *5* (2), No. e10153.
(161) Madathiparambil Visalakshan, R.; González García, L. E.; Benzigar, M. R.; Ghazaryan, A.; Simon, J.; Mierczynska-Vasilev, A.; Michl, T. D.; Vinu, A.; Mailänder, V.; Morsbach, S.; et al. The influence of nanoparticle shape on protein corona formation. *Small* **2020**, *16* (25), 2000285.
(162) Da Silva-Candal, A.; Brown, T.; Krishnan, V.; Lopez-Loureiro, I.; Ávila-Gómez, P.; Pusuluri, A.; Pérez-Díaz, A.; Correa-Paz, C.; Hervella, P.; Castillo, J.; et al. Shape effect in active targeting of nanoparticles to inflamed cerebral endothelium under static and flow conditions. *J. Controlled Release* **2019**, *309*, 94−105.
(163) Fu, L.; Shi, B.; Wen, S.; Morsch, M.; Wang, G.; Zhou, Z.; Mi, C.; Sadraeian, M.; Lin, G.; Lu, Y.; et al. Aspect ratio of PEGylated upconversion nanocrystals affects the cellular uptake in vitro and in vivo. *Acta Biomater.* **2022**, *147*, 403−413.
(164) Stylianopoulos, T.; Poh, M.-Z.; Insin, N.; Bawendi, M. G.; Fukumura, D.; Munn, L. L.; Jain, R. K. Diffusion of particles in the extracellular matrix: the effect of repulsive electrostatic interactions. *Biophys. J.* **2010**, *99* (5), 1342−1349.
(165) Zhu, G.; Bian, Y.; Hursthouse, A. S.; Xu, S.; Xiong, N.; Wan, P. The role of magnetic MOFs nanoparticles in enhanced iron coagulation of aquatic dissolved organic matter. *Chemosphere* **2020**, *247*, 125921.
(166) Santa-Maria, A. R.; Walter, F. R.; Figueiredo, R.; Kincses, A.; Vigh, J. P.; Heymans, M.; Culot, M.; Winter, P.; Gosselet, F.; Dér, A.; Deli, M. A. Flow induces barrier and glycocalyx-related genes and negative surface charge in a lab-on-a-chip human blood-brain barrier model. *J. Cereb. Blood Flow Metab.* **2021**, *41* (9), 2201−2215.
(167) Gonzalez-Carter, D.; Goode, A. E.; Kiryushko, D.; Masuda, S.; Hu, S.; Lopes-Rodrigues, R.; Dexter, D. T.; Shaffer, M. S. P.; Porter, A. E. Quantification of blood−brain barrier transport and neuronal toxicity of unlabelled multiwalled carbon nanotubes as a function of surface charge. *Nanoscale* **2019**, *11* (45), 22054−22069.
(168) Li, H.; Zha, S.; Li, H.; Liu, H.; Wong, K. L.; All, A. H. Polymeric Dendrimers as Nanocarrier Vectors for Neurotheranostics. *Small* **2022**, *18* (45), 2203629.
(169) Zhang, L.; Fan, J.; Li, G.; Yin, Z.; Fu, B. M. Transcellular model for neutral and charged nanoparticles across an in vitro blood−brain barrier. *Cardiovasc. Eng. Technol.* **2020**, *11*, 607−620.
(170) Chen, Y.-P.; Chou, C.-M.; Chang, T.-Y.; Ting, H.; Dembélé, J.; Chu, Y.-T.; Liu, T.-P.; Changou, C. A.; Liu, C.-W.; Chen, C.-T. Bridging Size and Charge Effects of Mesoporous Silica Nanoparticles for Crossing the Blood−Brain Barrier. *Front. Chem.* **2022**, *10*, 931584.
(171) Xiao, W.; Wang, Y.; Zhang, H.; Liu, Y.; Xie, R.; He, X.; Zhou, Y.; Liang, L.; Gao, H. The protein corona hampers the transcytosis of transferrin-modified nanoparticles through blood−brain barrier and attenuates their targeting ability to brain tumor. *Biomaterials* **2021**, *274*, 120888.
(172) Kuo, Y.-C.; Yang, I. S.; Rajesh, R. Suppressed XIAP and cIAP expressions in human brain cancer stem cells using BV6-and GDC0152-encapsulated nanoparticles. *J. Taiwan Inst. Chem. Eng.* **2022**, *135*, 104394.
(173) Topal, G. R.; Mészáros, M.; Porkoláb, G.; Szecskó, A.; Polgár, T. F.; Siklós, L.; Deli, M. A.; Veszelka, S.; Bozkir, A. ApoE-targeting increases the transfer of solid lipid nanoparticles with donepezil cargo across a culture model of the blood−brain barrier. *Pharmaceutics* **2021**, *13* (1), 38.
(174) Zhang, S.-S.; Asghar, S.; Ye, J.-X.; Lin, L.; Ping, Q.-N.; Chen, Z.-P.; Shao, F.; Xiao, Y.-Y. A combination of receptor mediated transcytosis and photothermal effect promotes BBB permeability and the treatment of meningitis using itraconazole. *Nanoscale* **2020**, *12* (46), 23709−23720.
(175) Monaco, I.; Camorani, S.; Colecchia, D.; Locatelli, E.; Calandro, P.; Oudin, A.; Niclou, S.; Arra, C.; Chiariello, M.; Cerchia, L.; Comes Franchini, M. Aptamer functionalization of nanosystems for glioblastoma targeting through the blood−brain barrier. *J. Med. Chem.* **2017**, *60* (10), 4510−4516.
(176) Li, B.; Bai, Y.; Yion, C.; Wang, H.; Su, X.; Feng, G.; Guo, M.; Peng, W.; Shen, B.; Zheng, B. Single-Atom Nanocatalytic Therapy for Suppression of Neuroinflammation by Inducing Autophagy of Abnormal Mitochondria. *ACS Nano* **2023**, *17* (8), 7511−7529.
(177) Zhang, Q.; Yang, L.; Zheng, Y.; Wu, X.; Chen, X.; Fei, F.; Gong, Y.; Tan, B.; Chen, Q.; Wang, Y.; et al. Electro-responsive micelle-based universal drug delivery system for on-demand therapy in epilepsy. *J. Controlled Release* **2023**, *360*, 759−771.
(178) Nong, J.; Glassman, P. M.; Myerson, J. W.; Zuluaga-Ramirez, V.; Rodriguez-Garcia, A.; Mukalel, A.; Omo-Lamai, S.; Walsh, L. R.; Zamora, M. E.; Gong, X.; et al. Targeted Nanocarriers Co-Opting Pulmonary Intravascular Leukocytes for Drug Delivery to the Injured Brain. *ACS Nano* **2023**, *17* (14), 13121−13136.
(179) Yin, T.; Xie, W.; Sun, J.; Yang, L.; Liu, J. Penetratin peptide-functionalized gold nanostars: enhanced BBB permeability and NIR photothermal treatment of Alzheimer's disease using ultralow irradiance. *ACS Appl. Mater. Interfaces* **2016**, *8* (30), 19291−19302.
(180) Di Mauro, P. P.; Cascante, A.; Brugada Vilà, P. B.; Gómez-Vallejo, V.; Llop, J.; Borrós, S. Peptide-functionalized and high drug loaded novel nanoparticles as dual-targeting drug delivery system for modulated and controlled release of paclitaxel to brain glioma. *Int. J. Pharm.* **2018**, *553* (1−2), 169−185.
(181) Kuo, Y.-C.; Cheng, S.-J. Brain targeted delivery of carmustine using solid lipid nanoparticles modified with tamoxifen and lactoferrin for antitumor proliferation. *Int. J. Pharm.* **2016**, *499* (1−2), 10−19.
(182) Song, Y.; Du, D.; Li, L.; Xu, J.; Dutta, P.; Lin, Y. In vitro study of receptor-mediated silica nanoparticles delivery across blood−brain barrier. *ACS Appl. Mater. Interfaces* **2017**, *9* (24), 20410−20416.
(183) Ayer, M.; Schuster, M.; Gruber, I.; Blatti, C.; Kaba, E.; Enzmann, G.; Burri, O.; Guiet, R.; Seitz, A.; Engelhardt, B.; Klok, H.-A. T Cell-Mediated Transport of Polymer Nanoparticles across the Blood−Brain Barrier. *Adv. Healthcare Mater.* **2021**, *10* (2), 2001375.
(184) Jeon, S. G.; Cha, M.-Y.; Kim, J.-i.; Hwang, T. W.; Kim, K. A.; Kim, T. H.; Song, K. C.; Kim, J.-J.; Moon, M. Vitamin D-binding protein-loaded PLGA nanoparticles suppress Alzheimer's disease-related pathology in 5XFAD mice. *Nanomed.: Nanotechnol. Biol. Med.* **2019**, *17*, 297−307.
(185) Chung, E. P.; Cotter, J. D.; Prakapenka, A. V.; Cook, R. L.; DiPerna, D. M.; Sirianni, R. W. Targeting small molecule delivery to the brain and spinal cord via intranasal administration of rabies virus glycoprotein (RVG29)-modified PLGA nanoparticles. *Pharmaceutics* **2020**, *12* (2), 93.
(186) Cano, A.; Ettcheto, M.; Chang, J.-H.; Barroso, E.; Espina, M.; Kühne, B. A.; Barenys, M.; Auladell, C.; Folch, J.; Souto, E. B.; et al. Dual-drug loaded nanoparticles of Epigallocatechin-3-gallate (EGCG)/Ascorbic acid enhance therapeutic efficacy of EGCG in a APPswe/PS1dE9 Alzheimer's disease mice model. *J. Controlled Release* **2019**, *301*, 62−75.
(187) Hoyos-Ceballos, G. P.; Ruozi, B.; Ottonelli, I.; Da Ros, F.; Vandelli, M. A.; Forni, F.; Daini, E.; Vilella, A.; Zoli, M.; Tosi, G.; et al. PLGA-PEG-ANG-2 nanoparticles for blood−brain barrier crossing: Proof-of-concept study. *Pharmaceutics* **2020**, *12* (1), 72.
(188) You, L.; Wang, J.; Liu, T.; Zhang, Y.; Han, X.; Wang, T.; Guo, S.; Dong, T.; Xu, J.; Anderson, G. J.; et al. Targeted brain delivery of rabies virus glycoprotein 29-modified deferoxamine-loaded nanoparticles reverses functional deficits in parkinsonian mice. *ACS Nano* **2018**, *12* (5), 4123−4139.
(189) Qu, M.; Lin, Q.; He, S.; Wang, L.; Fu, Y.; Zhang, Z.; Zhang, L. A brain targeting functionalized liposomes of the dopamine derivative N-3, 4-bis (pivaloyloxy)-dopamine for treatment of Parkinson's disease. *J. Controlled Release* **2018**, *277*, 173−182.
(190) Rehman, M.; Madni, A.; Shi, D.; Ihsan, A.; Tahir, N.; Chang, K. R.; Javed, I.; Webster, T. J. Enhanced blood brain barrier


https://doi.org/10.1021/acsnano.3c10674
*ACS Nano* 2024, 18, 1820−1845

permeability and glioblastoma cell targeting via thermoresponsive lipid nanoparticles. *Nanoscale* **2017**, *9* (40), 15434−15440.
(191) Jhaveri, A.; Deshpande, P.; Pattni, B.; Torchilin, V. Transferrin-targeted, resveratrol-loaded liposomes for the treatment of glioblastoma. *J. Controlled Release* **2018**, *277*, 89−101.
(192) Liang, M.; Gao, C.; Wang, Y.; Gong, W.; Fu, S.; Cui, L.; Zhou, Z.; Chu, X.; Zhang, Y.; Liu, Q.; et al. Enhanced blood−brain barrier penetration and glioma therapy mediated by T7 peptide-modified low-density lipoprotein particles. *Drug delivery* **2018**, *25* (1), 1652−1663.
(193) You, Y.; Yang, L.; He, L.; Chen, T. Tailored mesoporous silica nanosystem with enhanced permeability of the blood−brain barrier to antagonize glioblastoma. *J. Mater. Chem. B* **2016**, *4* (36), 5980−5990.
(194) Mo, J.; He, L.; Ma, B.; Chen, T. Tailoring particle size of mesoporous silica nanosystem to antagonize glioblastoma and overcome blood−brain barrier. *ACS Appl. Mater. Interfaces* **2016**, *8* (11), 6811−6825.
(195) Song, Z.; Liu, T.; Chen, T. Overcoming blood−brain barrier by HER2-targeted nanosystem to suppress glioblastoma cell migration, invasion and tumor growth. *J. Mater. Chem. B* **2018**, *6* (4), 568−579.
(196) Aguilera, G.; Berry, C. C.; West, R. M.; Gonzalez-Monterrubio, E.; Angulo-Molina, A.; Arias-Carrión, Ó.; Méndez-Rojas, M. Á. Carboxymethyl cellulose coated magnetic nanoparticles transport across a human lung microvascular endothelial cell model of the blood−brain barrier. *Nanoscale Adv.* **2019**, *1* (2), 671−685.
(197) Wu, D.; Qin, M.; Xu, D.; Wang, L.; Liu, C.; Ren, J.; Zhou, G.; Chen, C.; Yang, F.; Li, Y.; et al. A bioinspired platform for effective delivery of protein therapeutics to the central nervous system. *Adv. Mater.* **2019**, *31* (18), 1807557.
(198) Xiao, T.; He, M.; Xu, F.; Fan, Y.; Jia, B.; Shen, M.; Wang, H.; Shi, X. Macrophage membrane-camouflaged responsive polymer nanogels enable magnetic resonance imaging-guided chemotherapy/chemodynamic therapy of orthotopic glioma. *ACS Nano* **2021**, *15* (12), 20377−20390.
(199) Shen, Y.; Cao, B.; Snyder, N. R.; Woeppel, K. M.; Eles, J. R.; Cui, X. T. ROS responsive resveratrol delivery from LDLR peptide conjugated PLA-coated mesoporous silica nanoparticles across the blood−brain barrier. *J. Nanobiotechnol.* **2018**, *16* (1), 13.
(200) Deng, G.; Peng, X.; Sun, Z.; Zheng, W.; Yu, J.; Du, L.; Chen, H.; Gong, P.; Zhang, P.; Cai, L.; Tang, B. Z. Natural-killer-cell-inspired nanorobots with aggregation-induced emission characteristics for near-infrared-II fluorescence-guided glioma theranostics. *ACS Nano* **2020**, *14* (9), 11452−11462.
(201) Zha, S.; Wong, K. L.; All, A. H. Intranasal delivery of functionalized polymeric nanomaterials to the brain. *Adv. Healthcare Mater.* **2022**, *11* (11), 2102610.
(202) Zha, S.; Chau, H. F.; Chau, W. Y.; Chan, L. S.; Lin, J.; Lo, K. W.; Cho, W. C. S.; Yip, Y. L.; Tsao, S. W.; Farrell, P. J.; et al. Dual-Targeting Peptide-Guided Approach for Precision Delivery and Cancer Monitoring by Using a Safe Upconversion Nanoplatform. *Adv. Sci.* **2021**, *8* (5), 2002919.
(203) Zha, S.; Fung, Y. H.; Chau, H.-F.; Lin, J.; Wang, J.; Chan, L. S.; Zhu, G.; Lung, H. L.; Wong, K.-L.; Ma, P. Responsive upconversion nanoprobe for monitoring and inhibition of EBV-associated cancers via targeting EBNA1. *Nanoscale* **2018**, *10* (33), 15632−15640.
(204) Bao, G.; Wen, S.; Wang, W.; Zhou, J.; Zha, S.; Liu, Y.; Wong, K.-L.; Jin, D. Enhancing hybrid upconversion nanosystems via synergistic effects of moiety engineered NIR dyes. *Nano Lett.* **2021**, *21* (23), 9862−9868.
(205) Zha, S.; Matuszewska, C.; Wong, K.-L. Energy Transfer between Lanthanide to Lanthanide in Phosphors for Bioapplications. In *Phosphor Handbook*; CRC Press: 2022; pp 311−332.
(206) All, A. H.; Zeng, X.; Teh, D. B. L.; Yi, Z.; Prasad, A.; Ishizuka, T.; Thakor, N.; Hiromu, Y.; Liu, X. Expanding the toolbox of upconversion nanoparticles for in vivo optogenetics and neuromodulation. *Adv. Mater.* **2019**, *31* (41), 1803474.
(207) Zhang, Y.; Ma, X.; Chau, H.-F.; Thor, W.; Jiang, L.; Zha, S.; Fok, W.-Y.; Mak, H.-N.; Zhang, J.; Cai, J.; et al. Lanthanide−Cyclen−Camptothecin Nanocomposites for Cancer Theranostics Guided by Near-Infrared and Magnetic Resonance Imaging. *ACS Appl. Nano Mater.* **2021**, *4* (1), 271−278.
(208) Yi, Z.; Luo, Z.; Barth, N. D.; Meng, X.; Liu, H.; Bu, W.; All, A.; Vendrell, M.; Liu, X.; et al. Vivo Tumor Visualization through MRI Off-On Switching of NaGdF4−CaCO3 Nanoconjugates. *Adv. Mater.* **2019**, *31* (37), 1901851.
(209) Han, S.; Samanta, A.; Xie, X.; Huang, L.; Peng, J.; Park, S. J.; Teh, D. B. L.; Choi, Y.; Chang, Y. T.; All, A. H.; et al. Gold and hairpin DNA functionalization of upconversion nanocrystals for imaging and in vivo drug delivery. *Adv. Mater.* **2017**, *29* (18), 1700244.
(210) Peng, J.; Samanta, A.; Zeng, X.; Han, S.; Wang, L.; Su, D.; Loong, D. T. B.; Kang, N. Y.; Park, S. J.; All, A. H.; et al. Real-Time In Vivo Hepatotoxicity Monitoring through Chromophore-Conjugated Photon-Upconverting Nanoprobes. *Angew. Chem., Int. Ed.* **2017**, *56* (15), 4165−4169.
(211) Zeng, X.; Chen, S.; Weitemier, A.; Han, S.; Blasiak, A.; Prasad, A.; Zheng, K.; Yi, Z.; Luo, B.; Yang, I. H.; et al. Visualization of intraneuronal motor protein transport through upconversion microscopy. *Angew. Chem.* **2019**, *131* (27), 9363−9369.
(212) Liang, L.; Teh, D. B. L.; Dinh, N.-D.; Chen, W.; Chen, Q.; Wu, Y.; Chowdhury, S.; Yamanaka, A.; Sum, T. C.; Chen, C.-H.; et al. Upconversion amplification through dielectric superlensing modulation. *Nat. Commun.* **2019**, *10* (1), 1391.
(213) Huang, J.; Ye, W.; Zha, S.; Tao, Y.; Yang, M.; Huang, K.; Liu, J.; Fung, Y.-H.; Li, Y.; Li, P.; et al. Sensitive and responsive pentiptycene-based molecular fluorescence chemosensor for detection of polyamines. *J. Lumin.* **2021**, *232*, 117856.
(214) Chen, Q.; Wu, J.; Ou, X.; Huang, B.; Almutlaq, J.; Zhumekenov, A. A.; Guan, X.; Han, S.; Liang, L.; Yi, Z.; et al. All-inorganic perovskite nanocrystal scintillators. *Nature* **2018**, *561* (7721), 88−93.
(215) Chen, S.; Weitemier, A. Z.; Zeng, X.; He, L.; Wang, X.; Tao, Y.; Huang, A. J. Y.; Hashimotodani, Y.; Kano, M.; Iwasaki, H.; et al. Near-infrared deep brain stimulation via upconversion nanoparticle−mediated optogenetics. *Science* **2018**, *359* (6376), 679−684.
(216) Li, X.; Xie, C.; Zha, S.; Tam, W. S.; Jiang, M.; Wong, K. L. Biocompatible Porphyrin-Peptide Conjugates as Theranostic Agents Targeting the Epstein-Barr Virus. *ChemPlusChem.* **2022**, *87* (11), No. e202200184.
(217) Liu, X.; Wang, Y.; Li, X.; Yi, Z.; Deng, R.; Liang, L.; Xie, X.; Loong, D. T. B.; Song, S.; Fan, D.; et al. Binary temporal upconversion codes of Mn2+-activated nanoparticles for multilevel anti-counterfeiting. *Nat. Commun.* **2017**, *8* (1), 899.
(218) Liang, L.; Xie, X.; Loong, D. T. B.; All, A. H.; Huang, L.; Liu, X. Designing Upconversion Nanocrystals Capable of 745 nm Sensitization and 803 nm Emission for Deep-Tissue Imaging. *Chem. - Eur. J.* **2016**, *22* (31), 10801−10807.
(219) Duan, R.; Xu, Y.; Zeng, X.; Xu, J.; Liang, L.; Zhang, Z.; Wang, Z.; Jiang, X.; Xing, B.; Liu, B.; et al. Uncovering the metabolic origin of aspartate for tumor growth using an integrated molecular deactivator. *Nano Lett.* **2021**, *21* (1), 778−784.
(220) Ding, B.; Shao, S.; Yu, C.; Teng, B.; Wang, M.; Cheng, Z.; Wong, K. L.; Ma, P. a.; Lin, J. Large-pore mesoporous-silica-coated upconversion nanoparticles as multifunctional immunoadjuvants with ultrahigh photosensitizer and antigen loading efficiency for improved cancer photodynamic immunotherapy. *Adv. Mater.* **2018**, *30* (52), 1802479.
(221) Zha, S.; Yang, F.; Ma, Z.; Wu, H.; Zhang, D.; Li, D. Multifunctional upconversion nanocomposite for multi-purpose cancer theranostics. *Mater. Des.* **2023**, *226*, 111682.
(222) Zha, S.; Li, H.; Law, G.-L.; Wong, K.-L.; All, A. H. Sensitive and responsive upconversion nanoprobes for fluorescence turn-on detection of glucose concentration. *Mater. Des.* **2023**, *227*, 111800.
(223) Zha, S.; Pan, S.; Jian, Y.; Peng, Y.; Jiang, L. Ultrasensitive and rapid detection of hydrogen sulfide by an upconversion nanosensor


https://doi.org/10.1021/acsnano.3c10674
*ACS Nano* 2024, 18, 1820−1845

NaYF4: Yb3+, Tm3+@ NaYF4@ Ag2O. *Mater. Des.* **2024**, *237*, 112546.



https://doi.org/10.1021/acsnano.3c10674
*ACS Nano* 2024, 18, 1820−1845